01.01.98

Happy New Year!

BEAM DYNAMICS IN THE TAU FEL. SIMULATIONS BY NEW VERSION EGUN2-CODE

Sergey Efimov

INTRODUCTION

Using the new version of the code E-GUN (3.025) series of beam dynamics simulations for TAU FEL were done. There are first results of beam dynamics simulates for electron gun, accelerator and decelerator with focusing by means short solenoids led.

1. Beam dynamics in the TAU FEL electron gun.

1.1. Geometry of the gun was took from the electron gun drawing, but exterior spline radius of the grid electrode was changed from 9mm to 7.73mm because combinations of such sizes as: position of the grid electrode focus (z=138.5mm for z=0 on the cover of the cathode, that corresponds to size 137.5mm on the drawing), grid electrode focus radius 120mm, grid electrode exterior diameter in the radial direction 73mm and longitudinal size 21mm are not correctly. Note that this changing don't influences on the beam dynamic just a little.

1.2. Initial beam radius on the cathode is 7.6mm. Beam envelope, radial current density displacement and beam phase portrait are led in the Appendix (Fig.A1-Fig.A3 correspondingly). The calculating gun perveance for voltages between cathode and anode U_{ca} =43kV, between grid electrode and cathode U_{cg}=12kV p=0.19538 mkA/V$^{3/2}$ and average beam current I_{beam}= 1.7421A. For the same U_{cg} and U_{ca}=45kV p=0.18303, I_{beam}= 1.7472A. One of the intermediate result is following: for changing anode aperture from 12.7mm up to 22.7mm beam size on the point z=300mm is changed less then 3%.

1.3. Beam dynamics simulates for U_{ca} =70kV and the same potential of the grid (12kV) were did. Figures with electron rays trajectories, radial displacement of the beam current and phase portrait for this case are led in the Appendix (Fig.A4-Fig.A6).

1.4. Some simulates for different potentials of the grid were done. Results are shown on the Fig.1 and Fig.2 (U_{ca}=43kV).

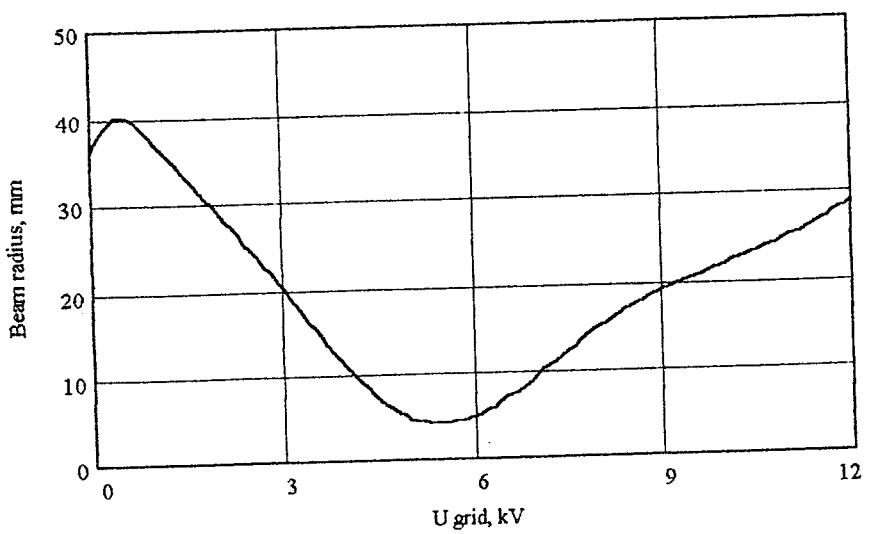

Fig.1.Dependence of the beam radius from grid potential for U_{ca}=45kV on the distance z=300mm from cathode.

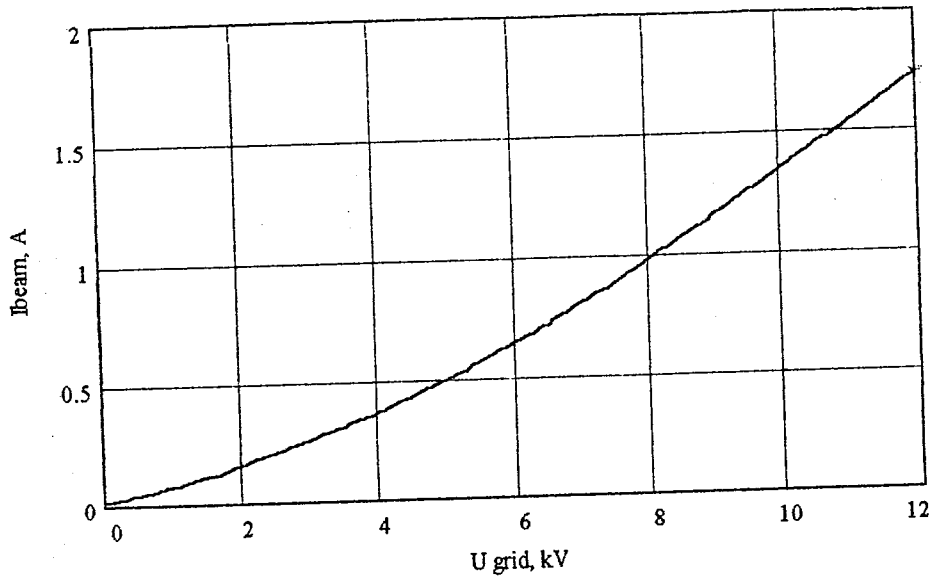

Fig.2. Dependence of the beam current from grid voltage for U_{ca} =45kV and z=300mm.

It may be shown if potential of the grid increases, beam current and beam radius increase also, but region with $U_{cg} \leq 8$ kV is not interesting consequently small beam current.

1.5. Beam dynamics in the electron gun for TAU FEL were simulated also in the Prudence Software Ltd. (Jerusalem, Director Boris Fomel) with using their new codes and almost the same results were received: for U_{ca} =43kV and U_{cg} =12kV perveance p=0.19408 mkA/V$^{3/2}$, beam radius 33mm.

2. Optimization of the beam injection in the accelerator.

2.1. Injection part structure of the TAU FEL is shown on the Fig.3. The

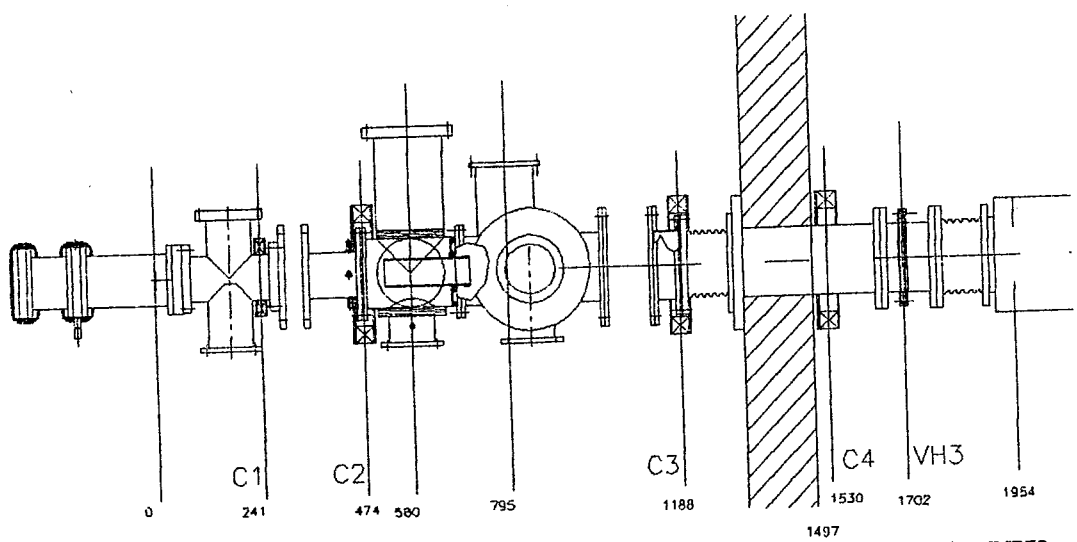

Fig.3. Injection part of the FEL TAU. C1-C4 - short focusing solenoids, VH3 - corrector, numbers below mean distance from cathode, stroked - wall of the tank.

first diagnostic screen is disposed on the distance 795mm from cathode. Results of the simulates and comparing with experimental data for different means of the currents in the solenoids C1 and C2 are led in the Report from 18.11.97. The good suitability between experiment and simulations takes place (except 2 points). For the following simulates current of the solenoids C1 and C2 was fixed on the levels 7.25A (1450A-turns) and -3.75A (1575A-turns) correspondingly. Change of the current sign in the C1 and C2 no change beam parameters on the first diagnostic screen.

2.2. For forming beam with small radius and *divergence* on the enter of accelerator solenoids C3 and C4 are used (their constructions are identical to construction of the solenoid C2). Simulates were done with high-voltage electrodes of the acceleration tube because they influence on the beam characteristics so much. The place of beam parameter observation - it is the diagnostic box which disposed after acceleration tube on the distance 310mm from the exit (z=4137mm). The basic means of C3 and C4 currents are 3A and ±2A correspondingly. On the diagnostic box in this case for "-" beam radius R=9.5mm, and if "+" R =10.5mm, but full *divergence* dR/dr (r - radial coordinate) is less for "+": 5.6mrad, for "-" 5.6mrad. Also radial beam density displacement to take into account important. The beam tracing and some beam characteristics for this case it may be seen in the Appendix on the Fig.B1-Fig.B6 (Change of the scale take place). Beam crossover is fined on the coordinate z=4740mm.

2.3. Beam radius and emittance are led below on the Fig.4, Fig5 - for I(C3)=var, I(C4)=const=2A. Beam density changing with solenoid C3 current is shown on the Fig.6.

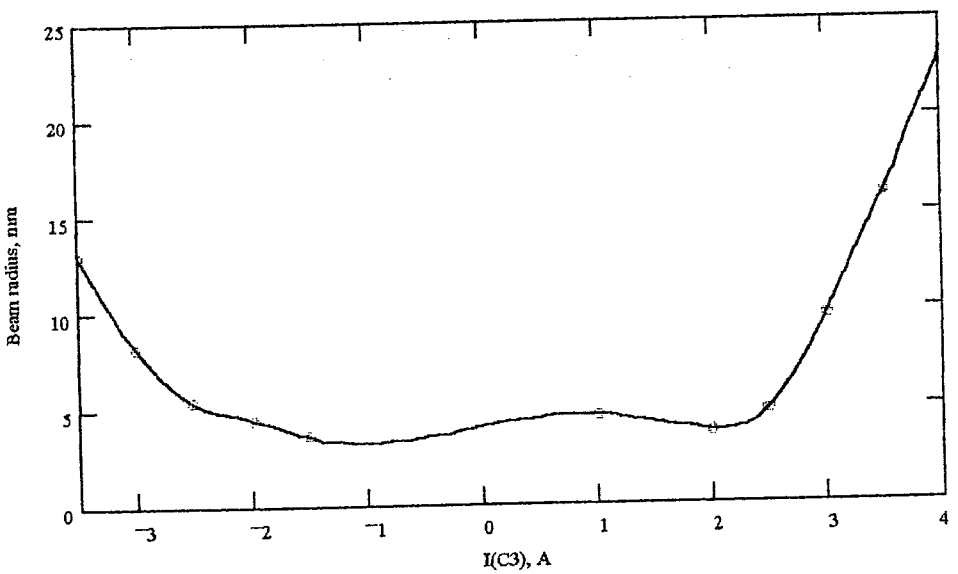

Fig.4. Dependence beam radius from solenoid C3 current for I(C4)=2A after accelerator on the first diagnostic box.

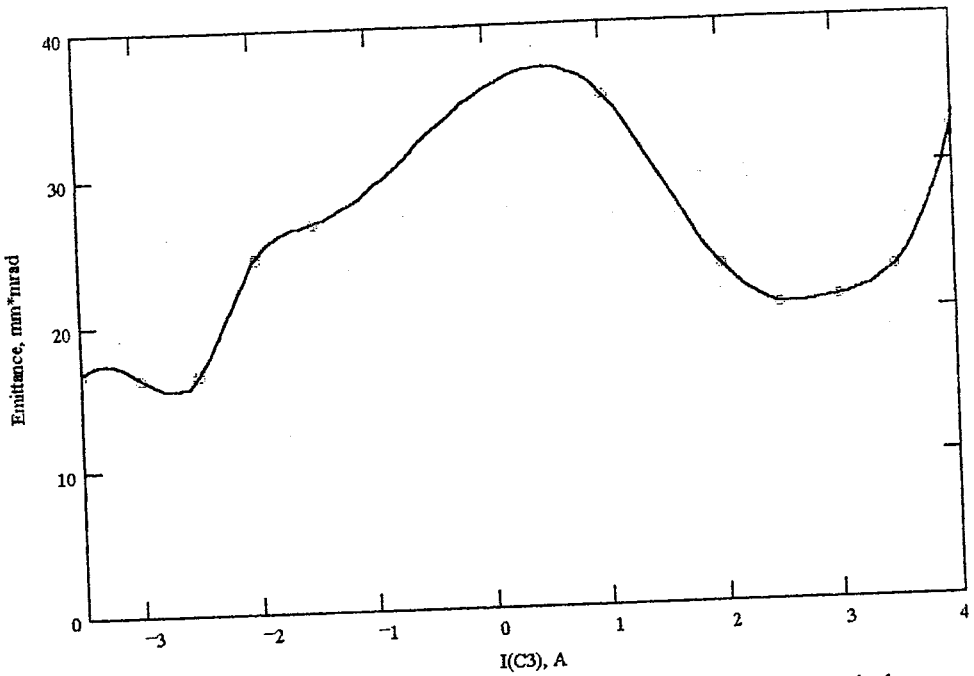

Fig.5. Emittance as the function of I(C3) on the first diagnostic box.

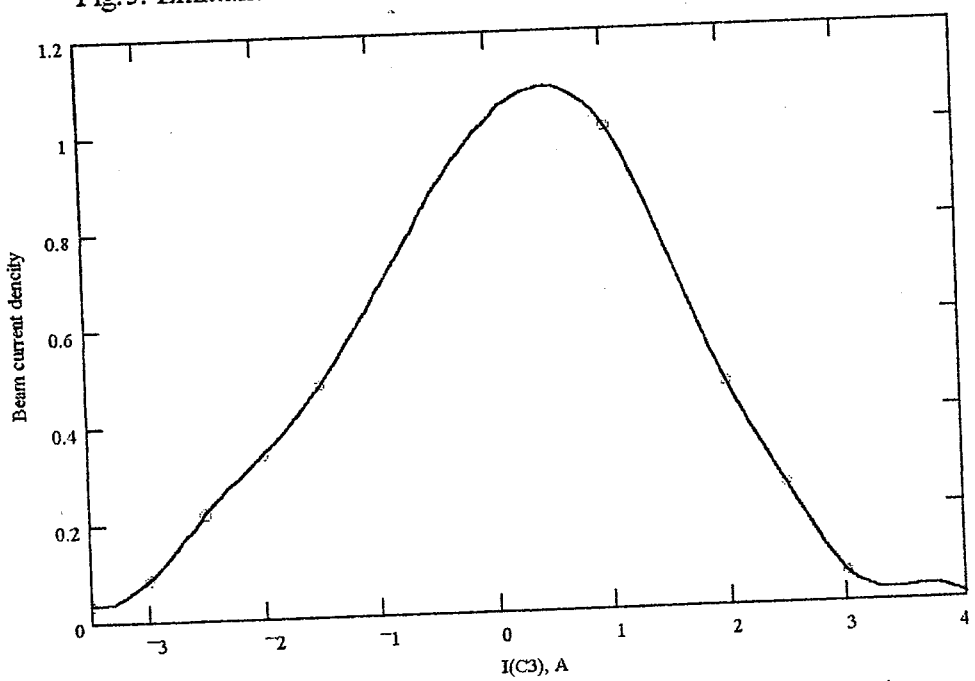

Fig.6. Change of average beam density with solenoid C3 current

Some comments.

-For I(C3)=0 and I(C3)= -1A one from 16 rays touch the first electrode of the accelerator.

- For means of the C3 current 1A, 2A and without current the maximum of the beam density lie near the beam axis.

-For I(C3)=2.5A tubing beam take place: maximum of the beam density is on the distance 0.6mm along radius, on the center density composes 0.15 from maximum.

-For I(C3)=3A density maximum places on the distance 3.5mm from axis and density on the axis consist 5% from maximum only.

- For 3.5A, 4A, 5A there is maximum of the beam density on the axis, but radial density displacement is characterized a big modulation. Also big modulation of the density take place for I(C3)= -2.5A, -3.5A.

Resume 1: The optimal mean of I(C3) is near ±2A for I(C4)=const=2A.

2.4. Results of simulations for case I(C3)=const=3A and I(C4)=var are shown below on the Fig.7.-Fig.9.

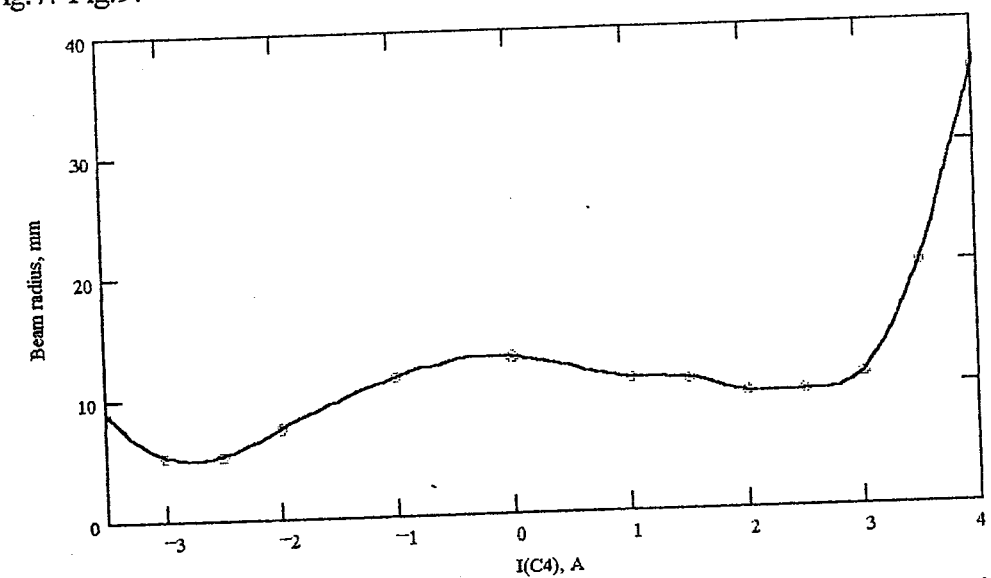

Fig.7. Beam radius on the first diagnostic box as function of solenoid C4 current for I(C3)=const=3A.

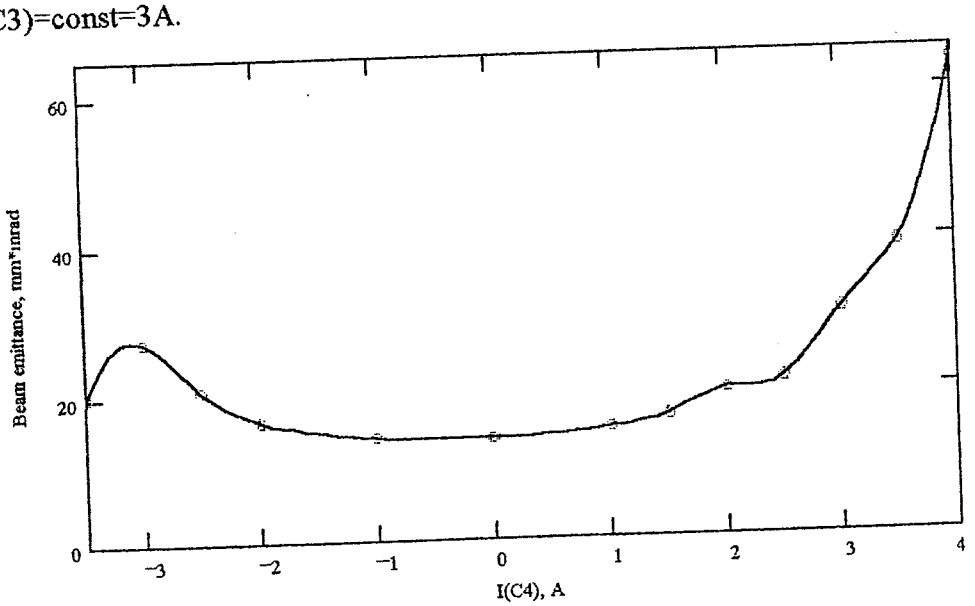

Fig.8. Dependence of the beam emittance from solenoid C4 current.

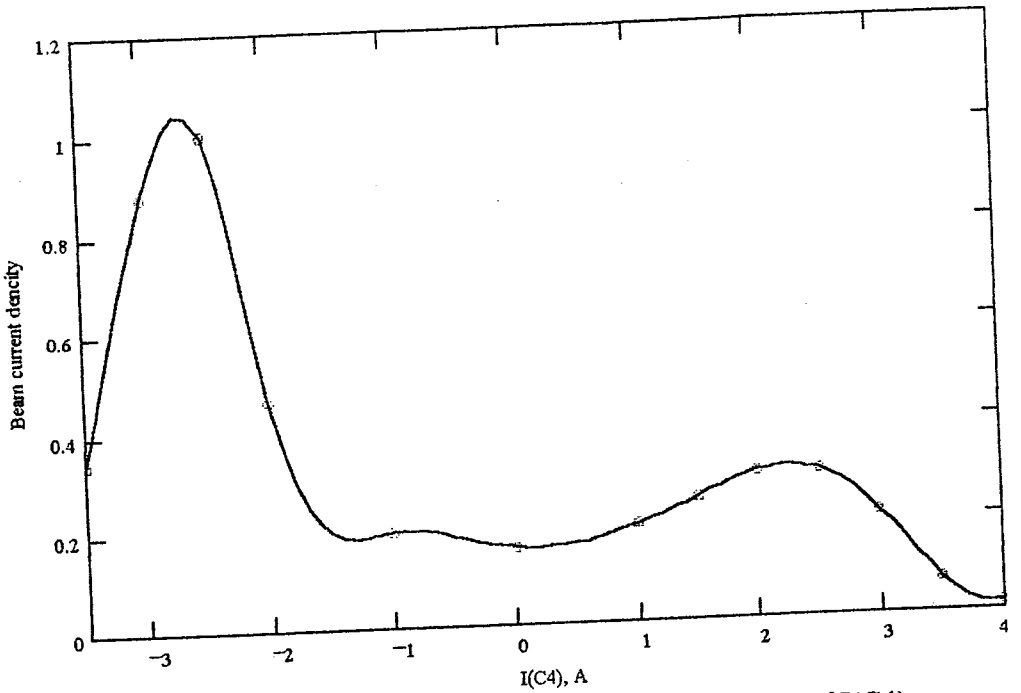

Fig.9. Relativistic average beam current density as function of I(C4).

2.5. Simulates for Ugun=70kV are shown that beam emittance after accelerator in this case is less noticeably, but perturbation of the one from 16 rays take place because it necessary to continue research of the beam stability in this regime.

Comments.

-The most large beam density near his axis - if I(C4)=2.5A.

-For I=1.5A, 3A, -2A - large oscillations of density along beam radius.

- For I(C4)= -2.5A - tubing of the beam. Maximum lies on the distance 0.6mm from axis.

Resume 2: For I(C3)=3A the beam parameters are optimally if I(C4)= -2.5A, but with a little tubing of the beam.

3. Model of acceleration structure.

3.1. The acceleration voltage in the tube is 1400kV, and with counting of the electron gun (45kV) beam energy after acceleration is 1445 kV.

3.2. It was difficult to input in the EGUN-code real forms of electrodes for acceleration and for deceleration. Because the simple model was used: the each electrode was submitted as the disk (rectangular to beam axis) with hole (radius R) for beam mowing and spline radius r=1.25mm (such thickness of the each electrode is equal to 2r). Displacement of potentials was determined from follow conditions:

- Full number of electrodes 75;
- The first and last pairs are shorting;
- The resistance between 2 and 3 electrodes is 100MOhm (appropriate to ΔU=5.622kV);
- Each resistance between 4 and 21 electrodes is 200MOhm (ΔU=11.245kV for each from 18 pairs);
- Each resistance between 22 and 74 electrodes is 400MOhm (ΔU=22.490kV for 53 pairs of electrodes).

3.3. There are data of electrodes of accelerator in the Table 1.

Table 1.

electrodes	1-8	9-14	15-21	22-27	28-32	33-37
R,mm	63.5	61.85	60.33	58.67	57.15	55.50

electrodes	38-42	42-47	48-52	53-57	58-64	65-69	70-75
R,mm	53.98	52.32	50.80	49.15	47.63	46.36	44.45

4. Model of decelerator.

4.1. Beam energy decrease in the deceleration section consist 1400keV and then beam energy on the collector enter is 45keV.

4.2. Displacement of potentials were done by follow conditions:

- Full number of electrodes is 80;
- One pair of the electrodes in the enter of tube and last 6 resistors are shorting;
- Resistance between each electrodes is 400MOhm, then ΔU=19.444kV for each pair;

4.3. There are data of electrodes of decelerator in the Table 2. Here numbering of electrodes is in opposition to beam direction.

Table 2.

des	1-6	7-11	12-16	17-19	20-22	23-25	26-28	29-31	32-34	35-37	38-40
R,mm	42.80	41.28	39.62	38.10	39.62	41.28	42.80	44.45	45.97	47.63	49.15

des	41-43	44-46	47-49	50-53	54-57	58-61	62-65	66-71	72-77	78-80
R,mm	50.80	52.32	53.98	55.50	57.15	58.67	60.33	61.85	63.50	38.10

5. Results of beam dynamics simulations in the decelerator section.

5.1. Goal of these simulations is to assemble beam in the collector without losses before. This part of the facility is led on the Fig. 10.

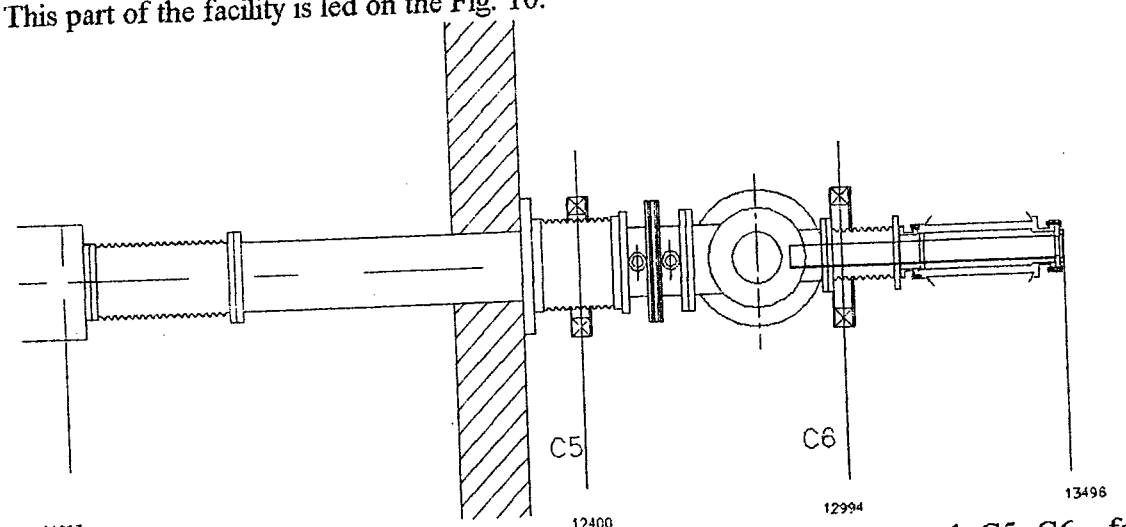

Fig.10. Part of the facility from last decelerator electrode up to end. C5, C6 - focusing short solenoids. Numerical mean distance from cathode.

5.2. Effectively of beam transport up to collector may be achieved by means C5 and C6 lens regimes (their construction s are the same as C2, C3, and C4 lenses) and initial beam

parameters on the decelerator tube enter. Beam initial parameters were make into account the same as beam parameters after acceleration section and any changes were made without change of emittance, because beam transport from exit of accelerator up to enter of decelerator was simulated without beam energy changing including loss energy on radiation.

5.2. One of beam dynamics simulates result is shown in the appendix on the Fig.D1-Fig.D3 (second half of the beam channel). Means of currents are I(C5)=4A, I(C6)= -4A. You can see that lens C5 acts on the part of the beam very strong, but on the part another - very weak.

5.3. Beam traces after initial beam condition changing are led in the appendix on the Fig.C4-Fig.C9 (pictures with scale for two parts of structure). Here beam radius is multiplied on 2 and divergence is devided on 2 (emittance is constant). Beam envelope is better, but not enough. It take place beam losses before and after lens C5. Also you can see that to decrease initial beam divergence (to increase it size) impossible without emittance changes.

5.5. Little changes of the high-voltage potential displacement along acceleration and deceleration section no essential if full potential is without changes.

6. Conclusion.

The first beam line optimization results for TAU- FEL using new EGUN-code are received. Currents in the lenses for beam tracing are obtain. But beam parameters in the collector is not satisfactory enough. Ways for beam parameter improvement may be follows:

-To decrease beam emittance in the acceleration part means of increasing electron gun voltage; insertion of energy losses in the wiggler due to radiation in the simulates; receiving more optimal currents for lenses in the injection of acceleration part.

- To determinate most optimal position for lenses, essentially near the collector.

- Previously at all - to determinate requirements to beam parameters on the enter of decelerator for effective beam tracing up to collector.

Appendix A

Electron gun.

Uac=43kV, Ugrid=12kV

Fig. A1. Beam tracing up to z=300mm

Fig. A2. Current density disrlacement for z=300mm.

Fig. A3. Beam on the phase plate.

Uac=70kV

Fig. A4. Beam tracing .

Fig.A5. Current density displacement.

Fig.A6. Beam on the phase plate

EGN: 3.825

e-gun TAU FEL
without solenoids.

p = 0.19538

ϕanode = 12.7 mm.

30.11.97.

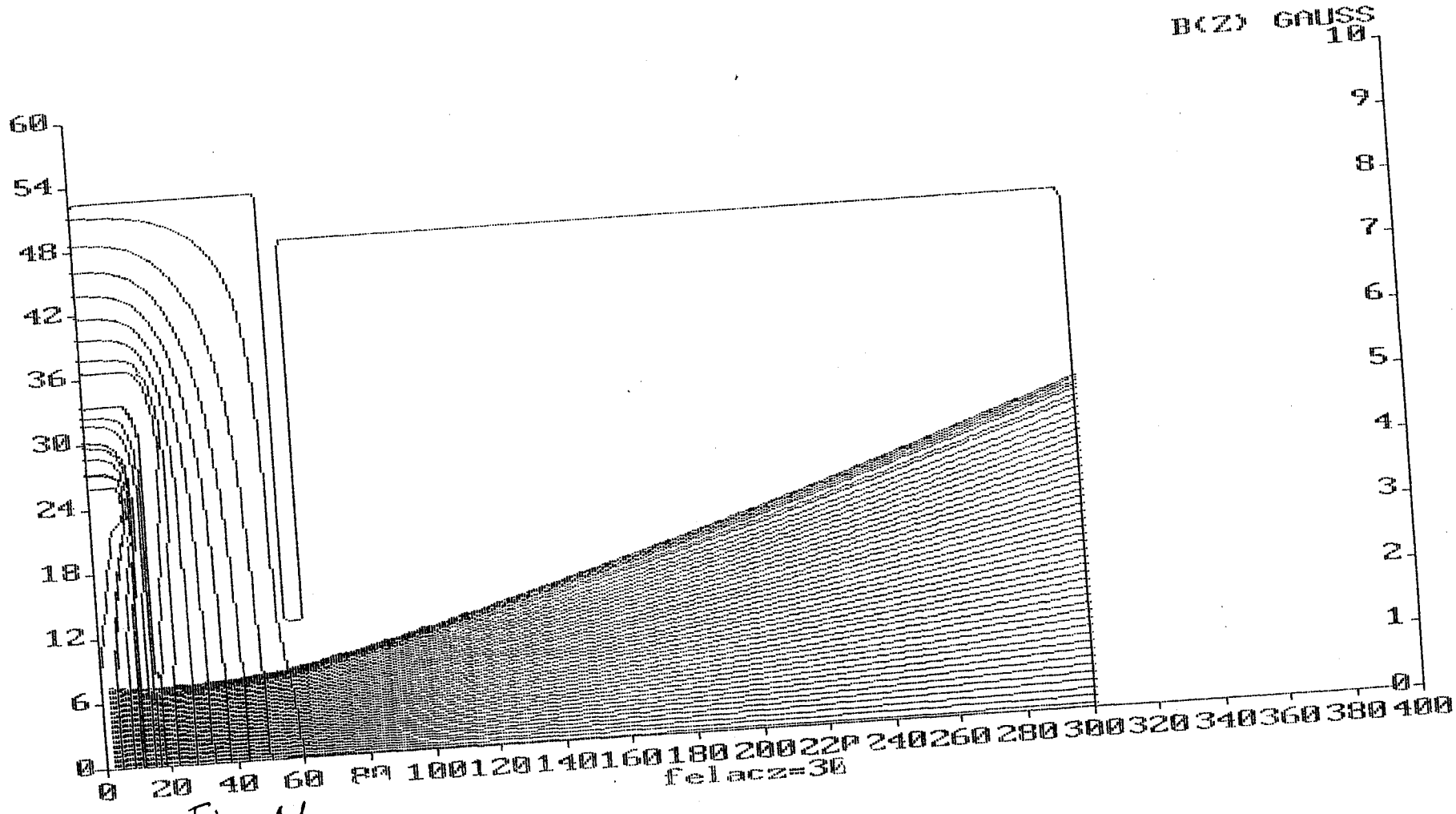

Fig. A1

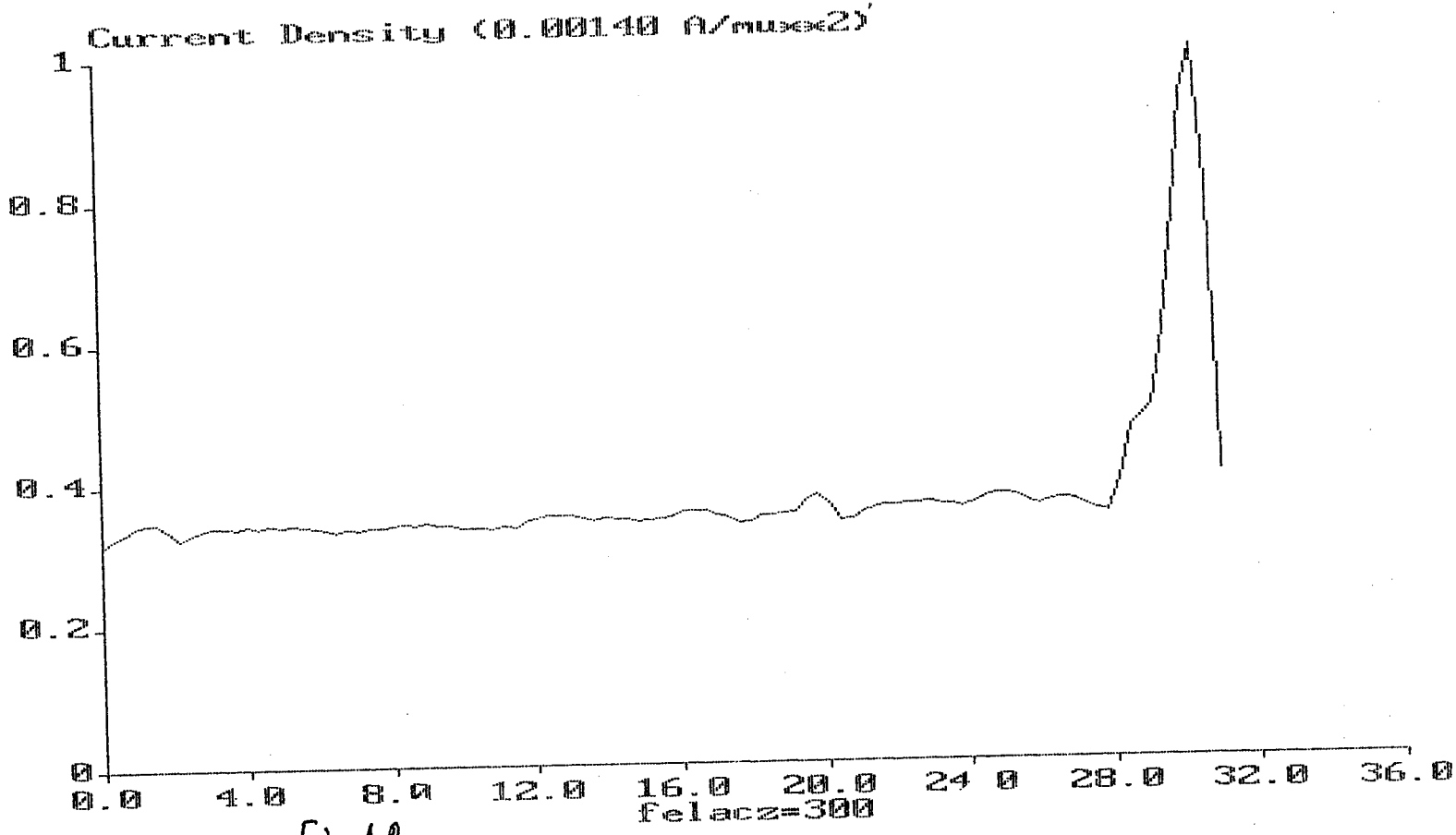
Current Density (0.00140 A/mu<2)
1
0.8
0.6
0.4
0.2
0
0.0
4.0
8.0
12.0
16.0
20.0
24 0
28.0
32.0
36.0
Felacz=300

Fig A2

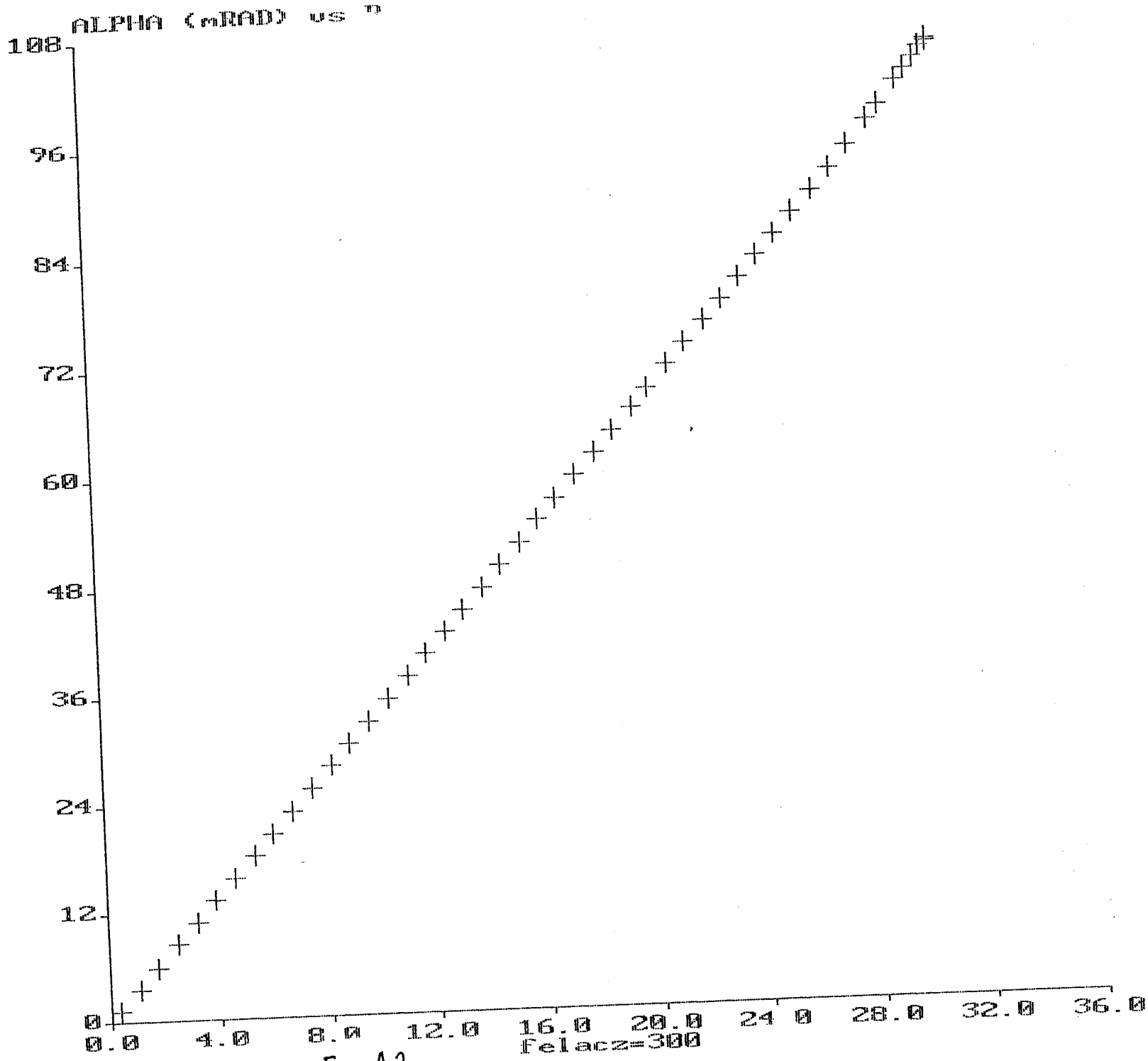
ALPHA (mRAD) vs
108
96
84
72
60
48
36
24
12
0
0.0
4.0
8.0
12.0
16.0
20.0
24.0
28.0
32.0
36.0
Felacz=300

Fig. A3.

Egun = 3.0 kV

$U_{grid} = 12\,kV$

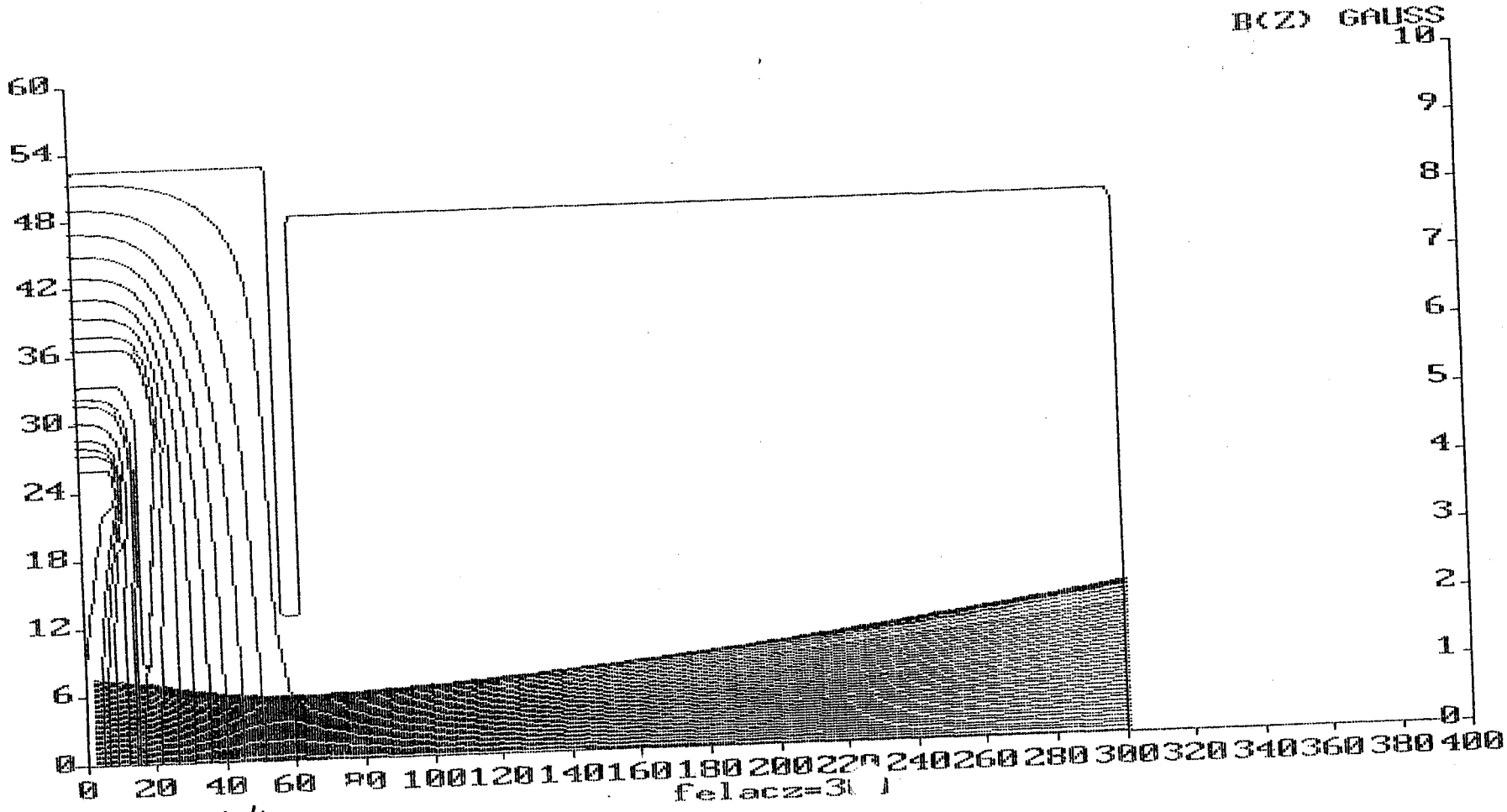

Fig. A 4

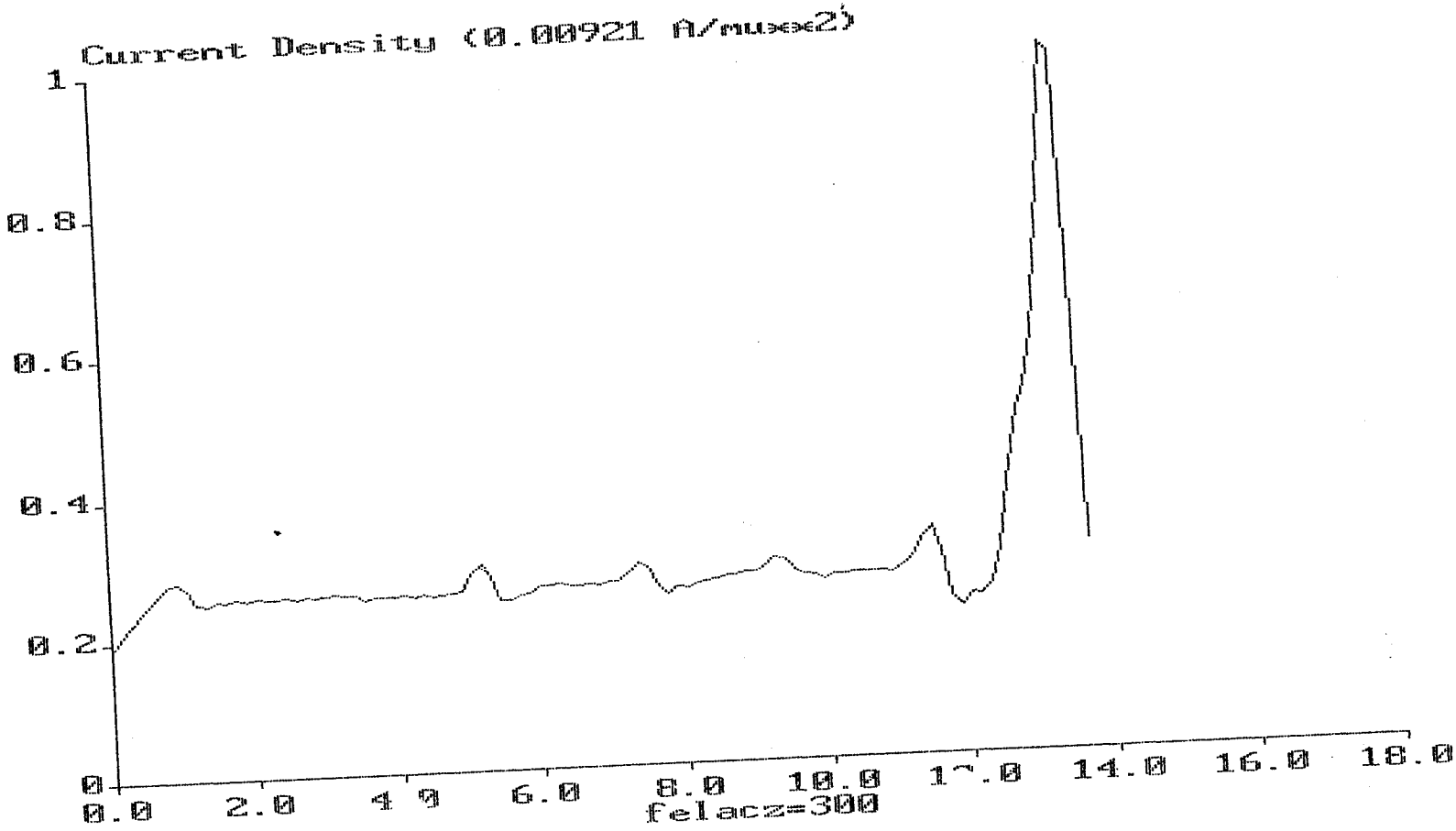
Current Density (0.00921 A/mu<<2)
1
0.8
0.6
0.4
0.2
0
0.0
2.0
4.0
6.0
8.0
10.0
12.0
14.0
16.0
18.0
felacz=300

Fig 45

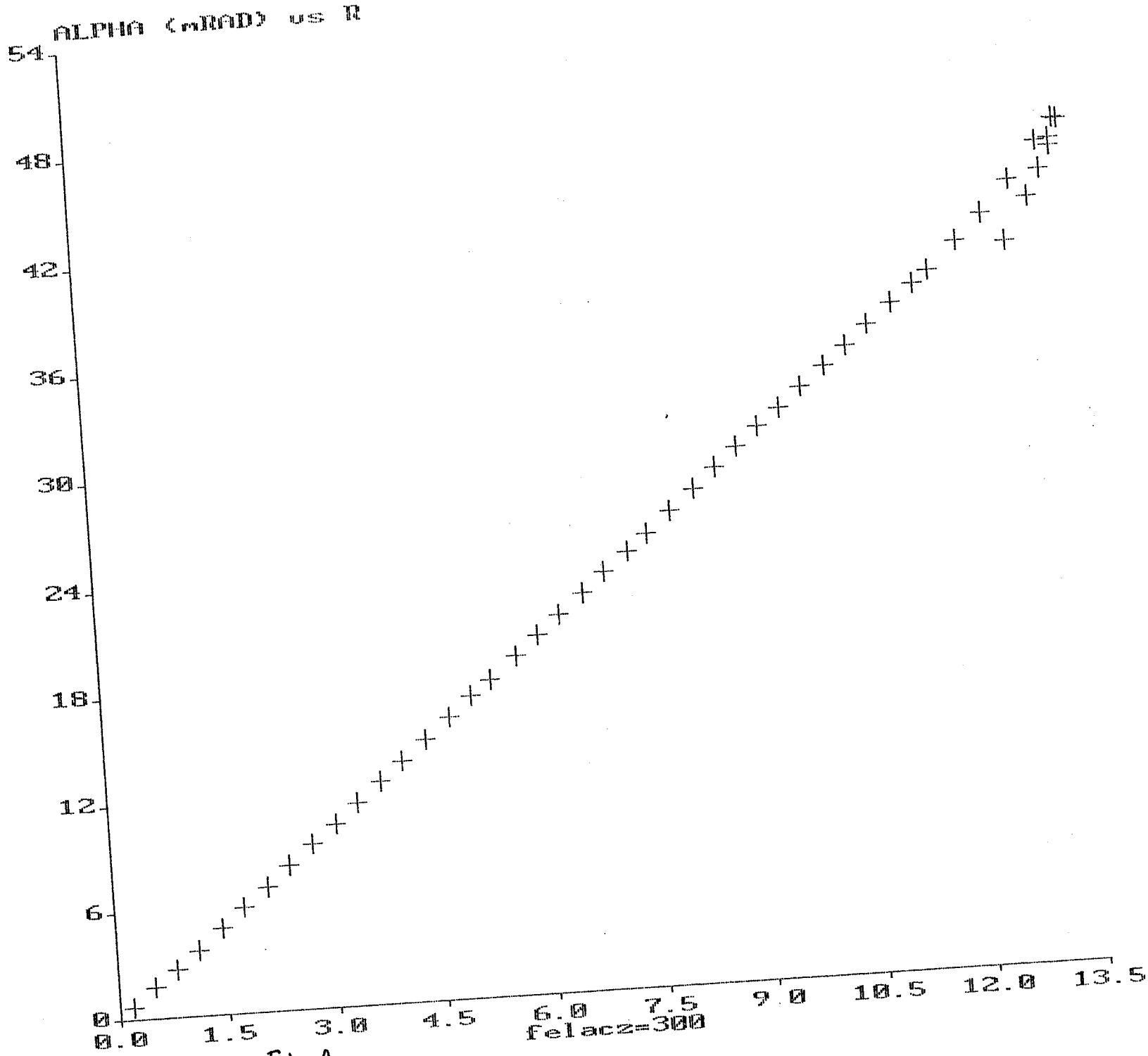
ALPHA (mRAD) vs R
54
48
42
36
30
24
18
12
6
0
0.0
1.5
3.0
4.5
6.0
7.5
9.0
10.5
12.0
13.5
felacz=300

Fig. A6.

Appendix B

Injection and acceleration.

E=45keV(gun)+1400keV(accelerator), I(C1)=7.25A, I(C2)=-3.75A, I(C3)=3A, I(C4)=2A

Fig.B1. Beam envelope up to z=3140mm.

Fig.B2. Current density displacement for z=3140mm

Fig.B3. Beam phase portrait for z=3140mm

Fig.B4. Beam envelope up to first diagnostic box (z=4137mm)

Fig.B5. Current density displacement for z=4137mm.

Fig.B6. Beam phase portrait for z=4137mm.

Solenoids : 7.25A, -3.75A, 3A, 2A.

17.12.97.

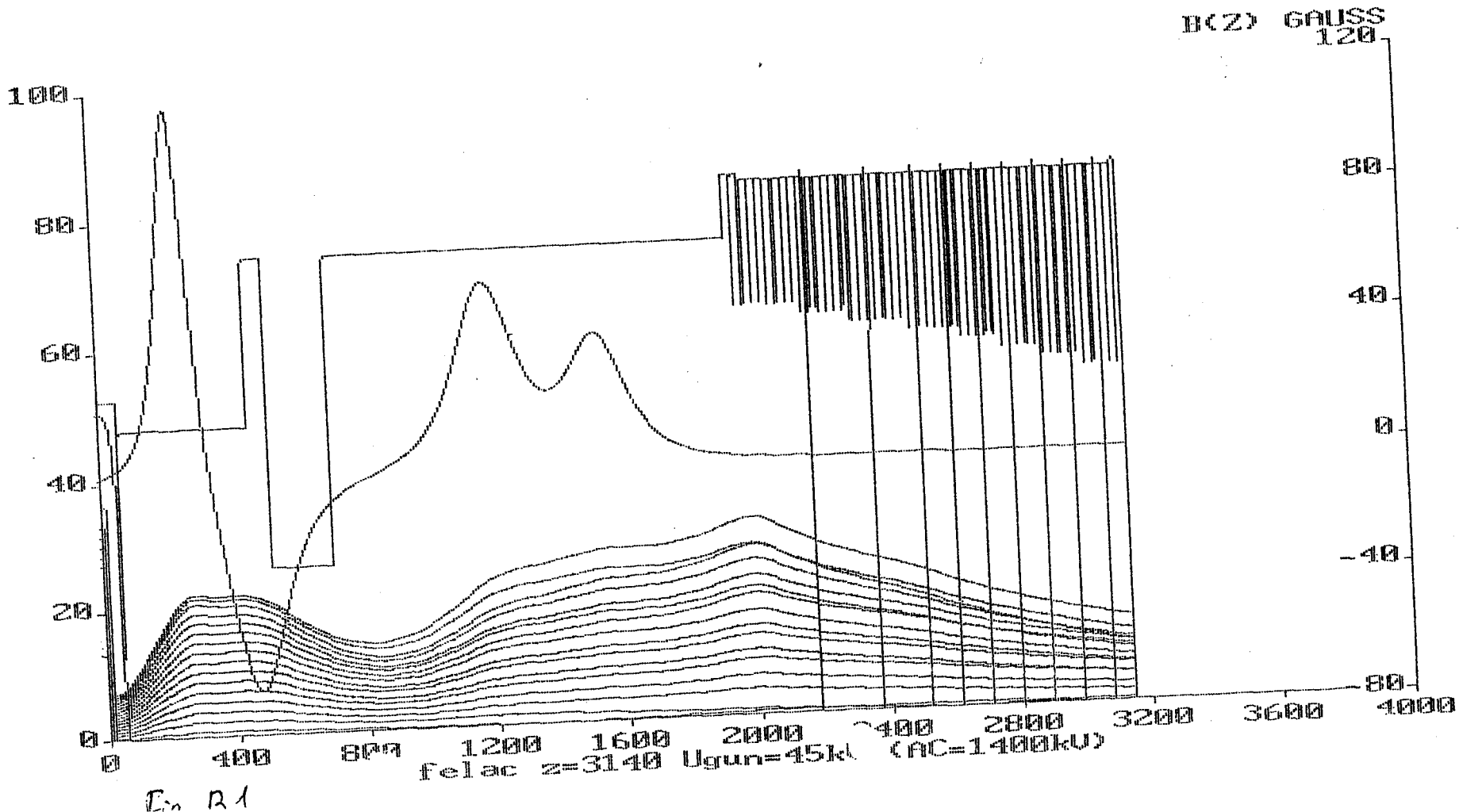

Fig B1

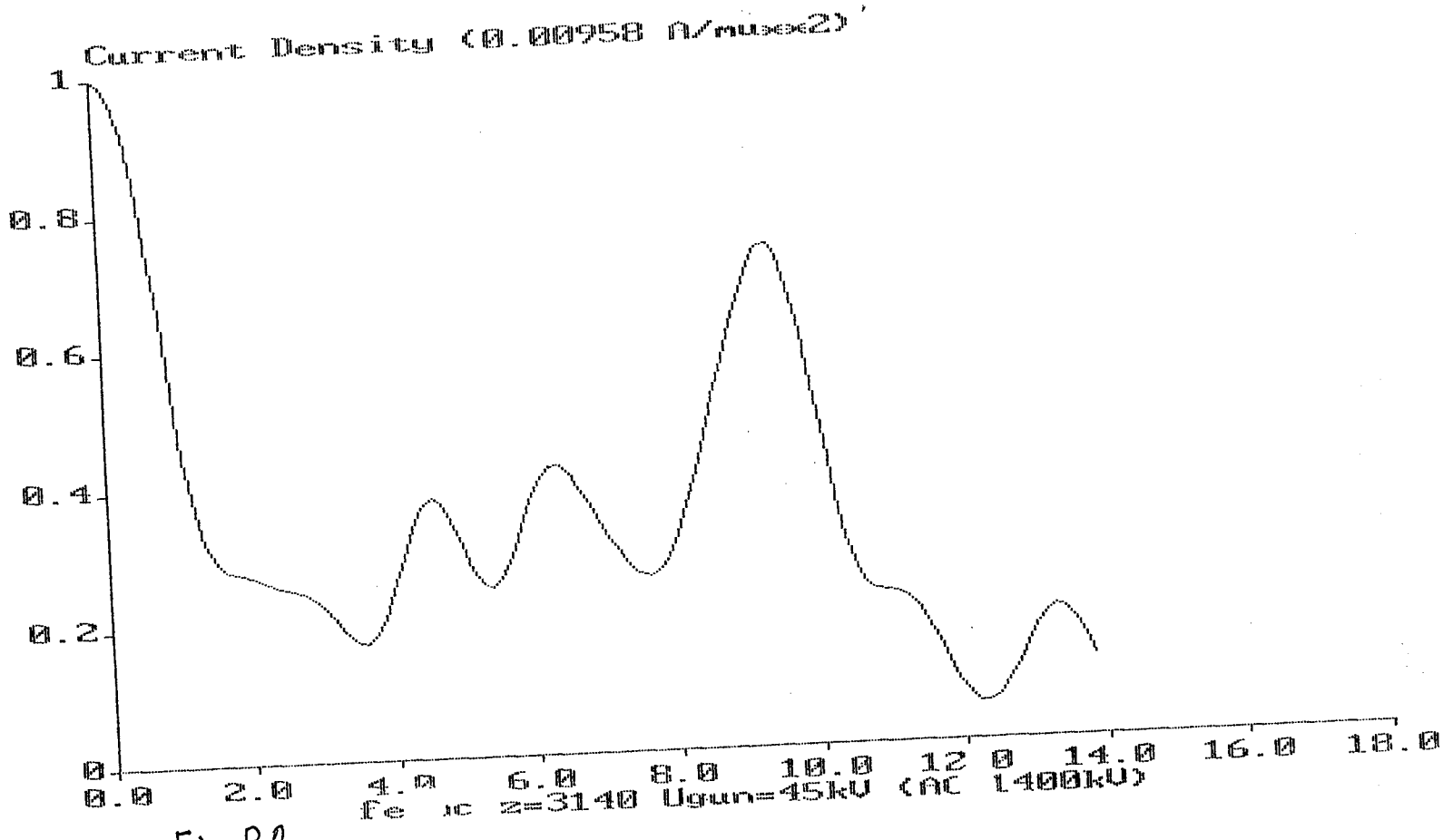
Current Density (0.00958 A/mu=x2)
1
0.8
0.6
0.4
0.2
0
0.0
2.0
4.0
6.0
8.0
10.0
12.0
14.0
16.0
18.0
Fe uc Z=3140 Ugun=45kV (AC 1400kV)

Fig B2

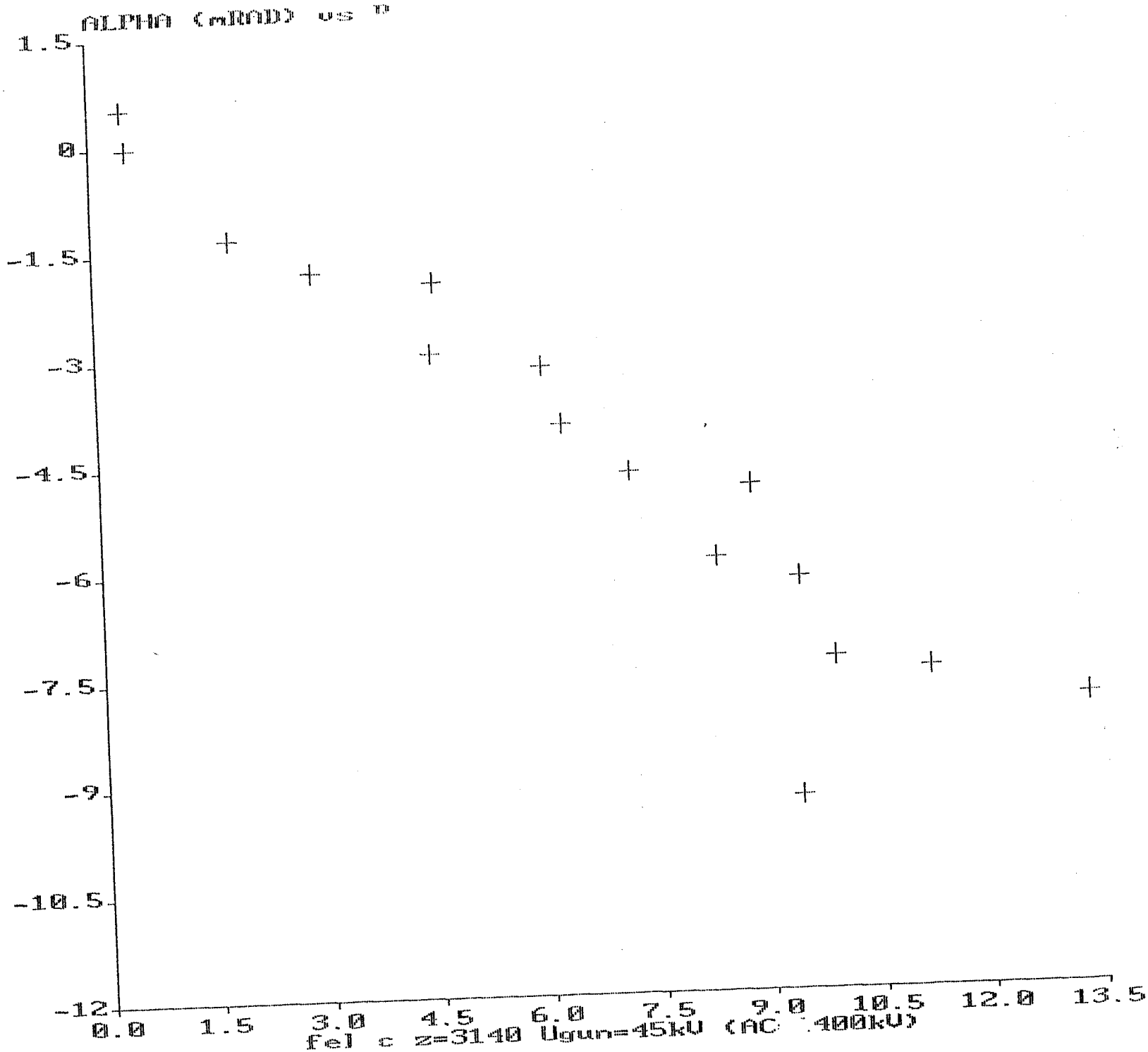
ALPHA (mRAD) vs
1.5
0
-1.5
-3
-4.5
-6
-7.5
-9
-10.5
-12
0.0
1.5
3.0
4.5
6.0
7.5
9.0
10.5
12.0
13.5
Fel c z=3140 Ugun=45kU (AC 400kU)

Fig 2.3

EGN: 3.025

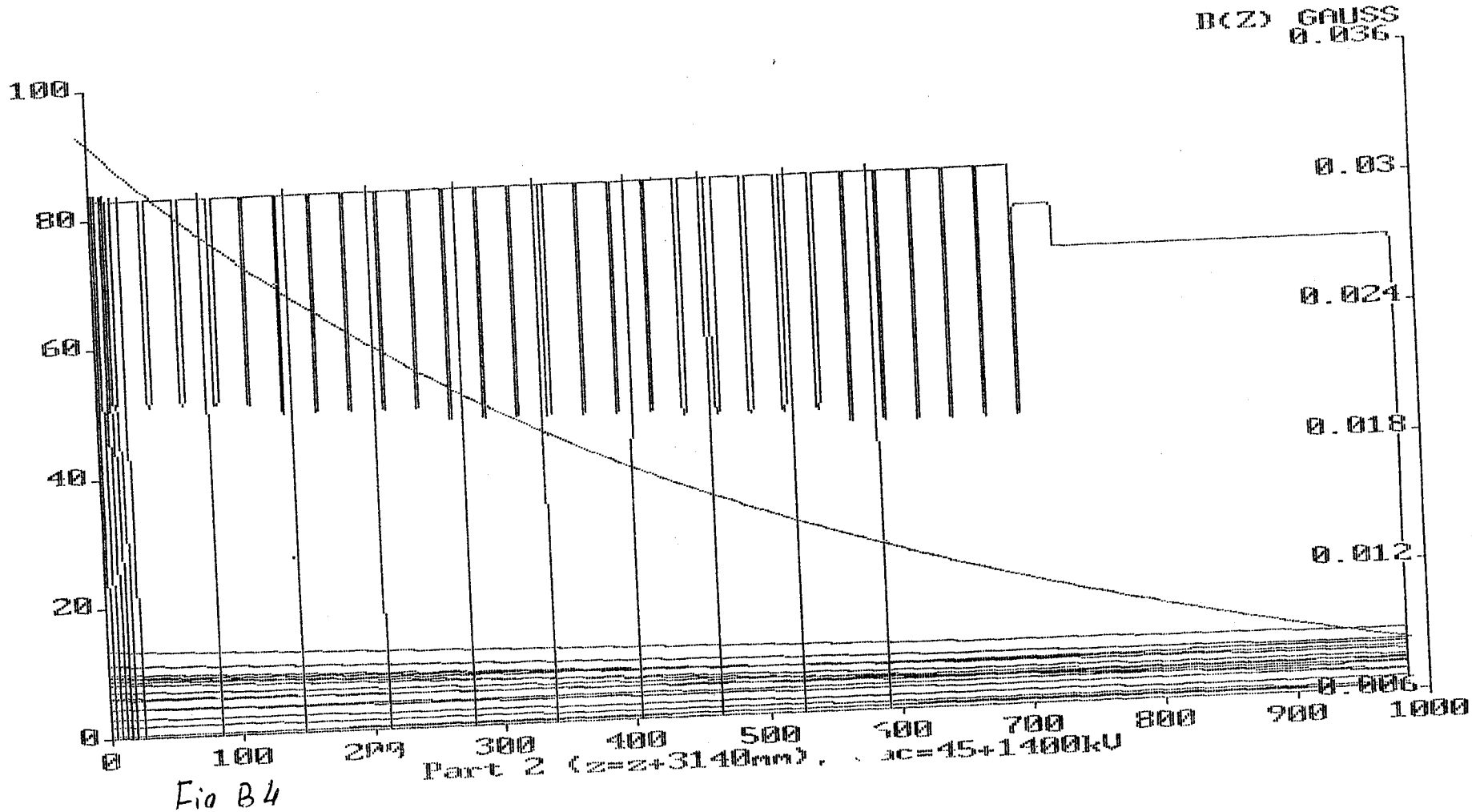

Fig B4

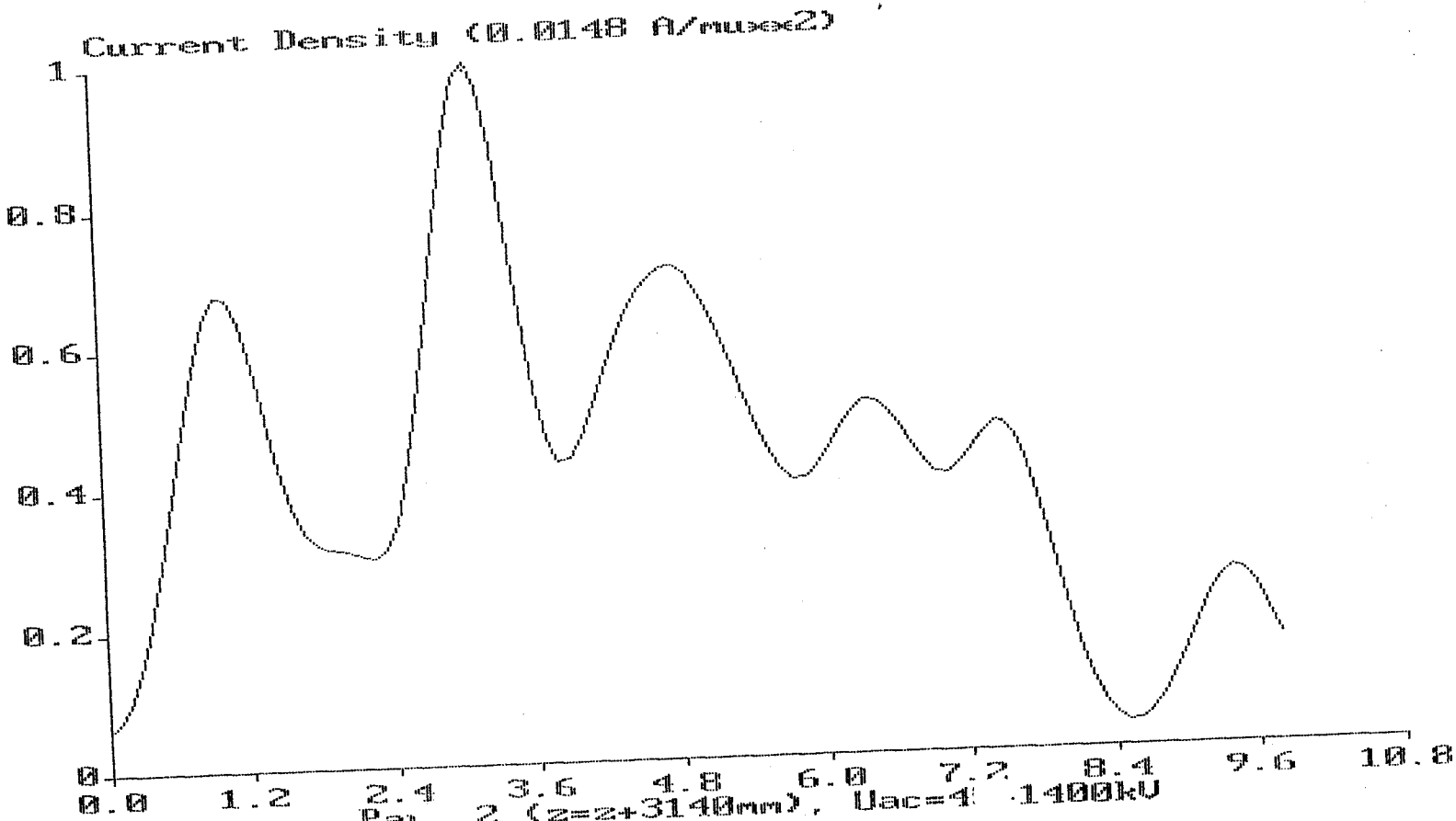
Current Density (0.0148 A/mu*e2)
1
0.8
0.6
0.4
0.2
0
0.0
1.2
2.4
3.6
4.8
6.0
7.2
8.4
9.6
10.8
Pa
2 (z=z+3140mm), Uac=4
.1400kU

Fig. B.5

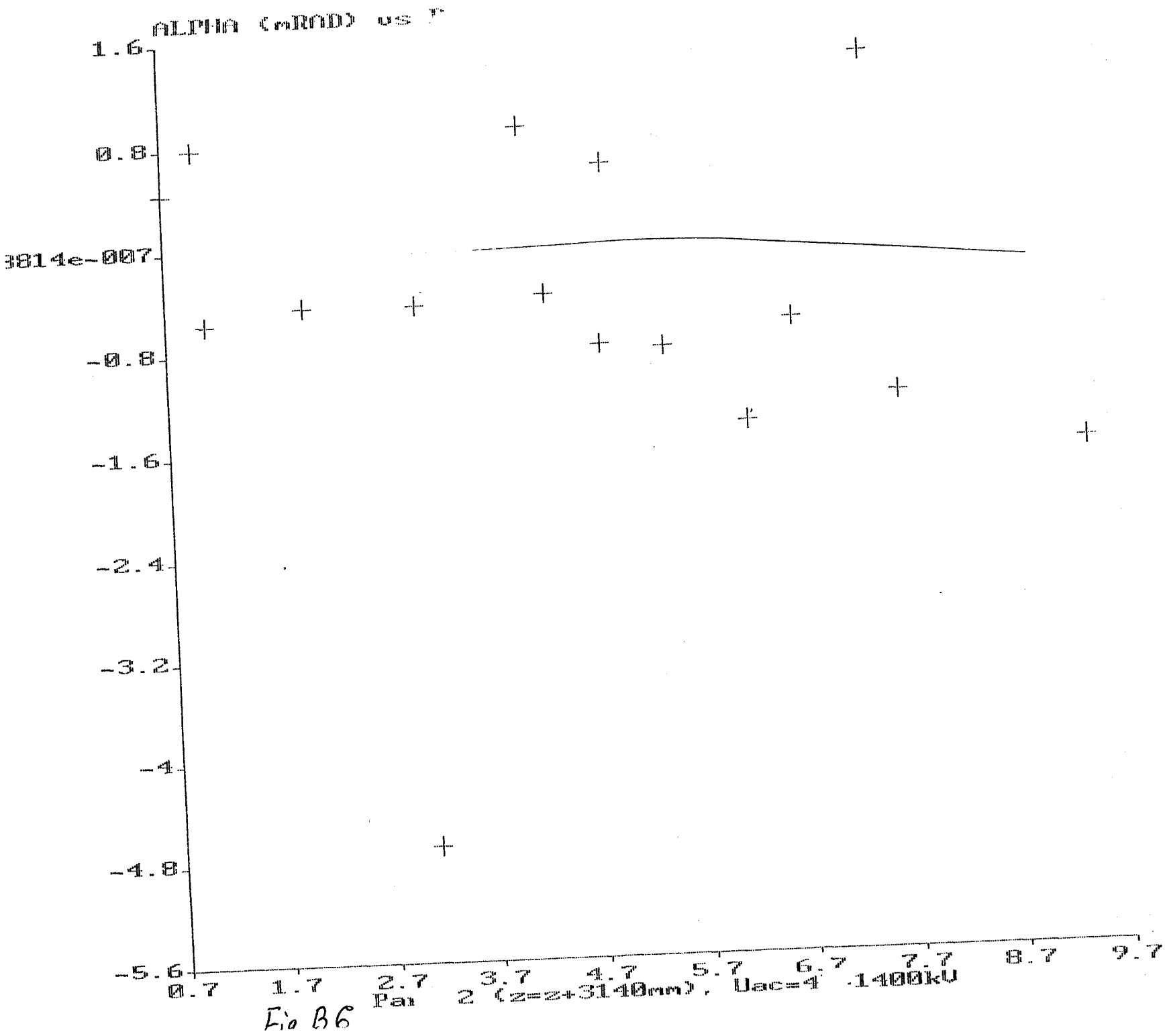
ALPHA (mRAD) vs
1.6
0.8
3814e-007
-0.8
-1.6
-2.4
-3.2
-4
-4.8
-5.6
0.7
1.7
2.7
3.7
4.7
5.7
6.7
7.7
8.7
9.7
Pas
2 (z=z+3140mm), Uac=4 .1400kU

Fig B6

Appendix C

Decelerator and collector.

E=1400keV(decelerator)+45keV(collector), I(C5)=4A, I(C6)= -4A.

There are initial beam parameters as in the first diagnostic box after accelerator if r-coordinate of each ray is increased by 2 and r' is decreased by 2.

Fig. C1. Beam tracing from enter of decelerator up to z=9147.3mm.

Fig. C2. Current density displacement for z=9147.3mm.

Fig. C3. Beam phase portrait for z=9147.3mm

Fig.C4-Fig.C6. The same as above but for end of the collector and all facility (z=13496mm).

Fig.C7-Fig.C9. Beam tracing across second part of decelerator and their parameters on the collector correspondingly for initial beam parameters without any changing.

EGN: 3.825

$r_{oi} = r_{oi} * 2$

$r'_{oi} = r'_{oi} / 2.$

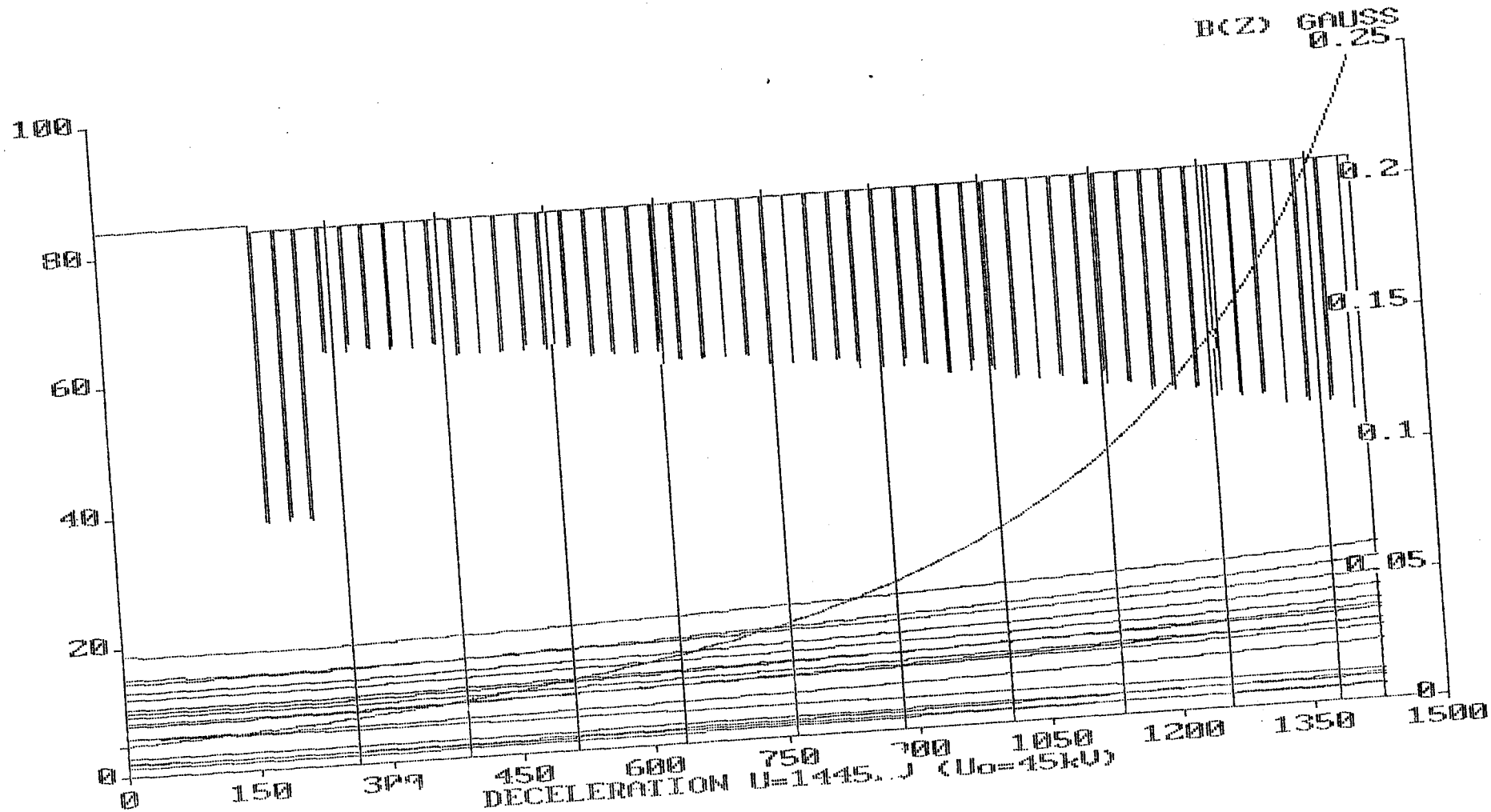

Fig. 61

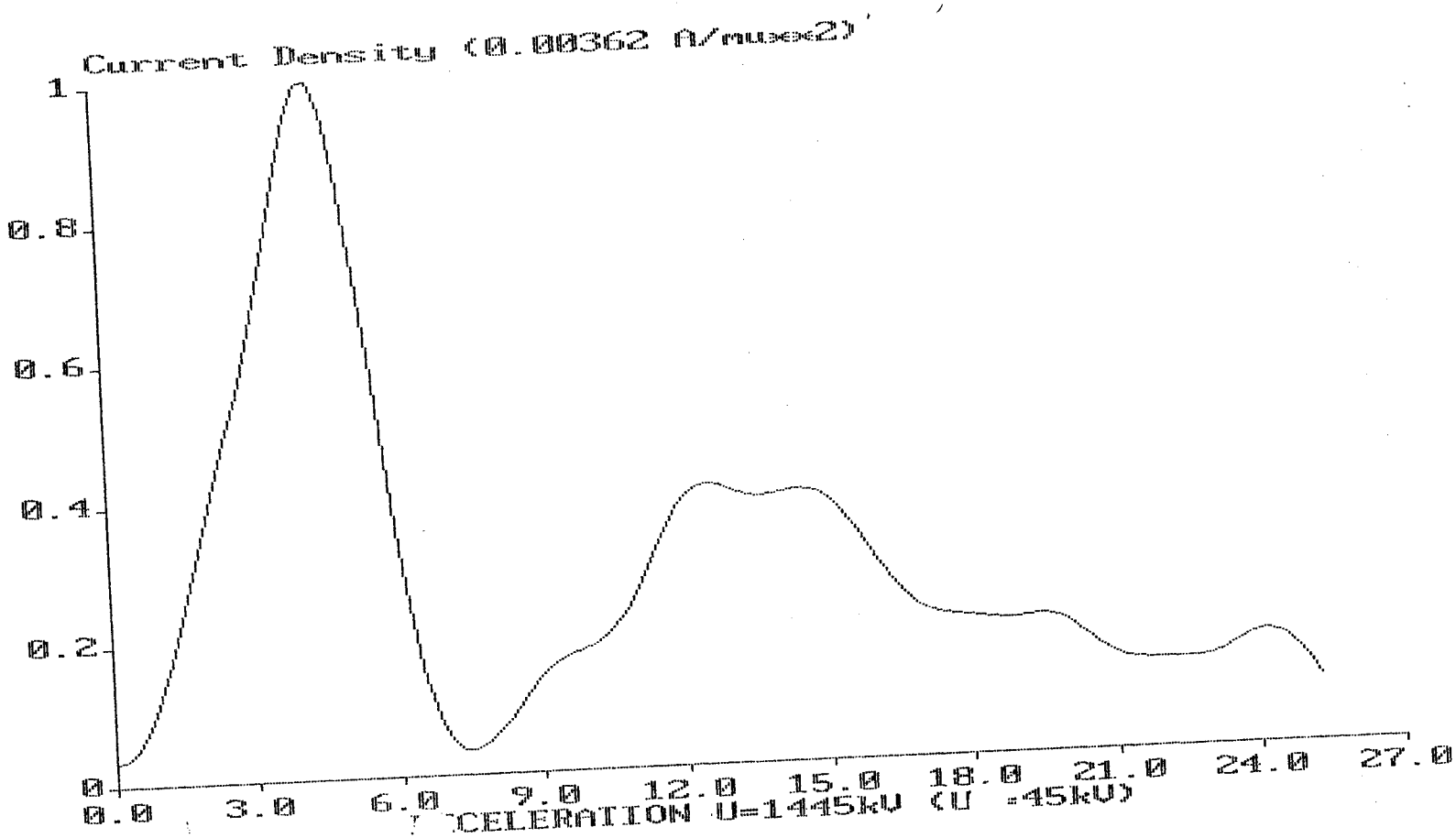
Current Density (0.00362 A/mu**2)
1
0.8
0.6
0.4
0.2
0
0.0
3.0
6.0
9.0
12.0
15.0
18.0
21.0
24.0
27.0
ACCELERATION U=145kV (U =45kV)

Fig. C2

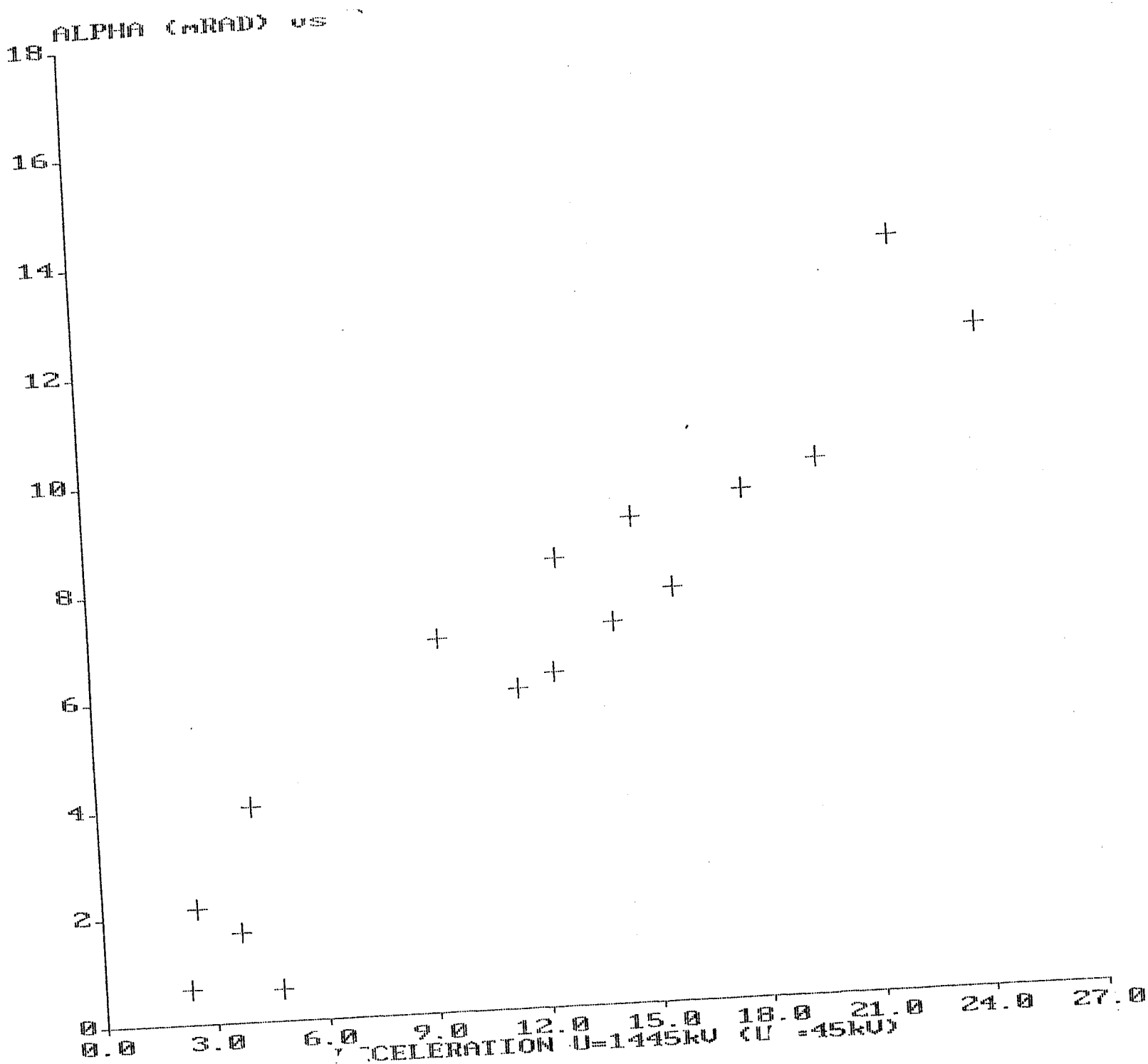
ALPHA (mRAD) vs
18
16
14
12
10
8
6
4
2
0
0.0
3.0
6.0
9.0
12.0
15.0
18.0
21.0
24.0
27.0
ACCELERATION U=1445kV (U =45kV)

Fig. C3

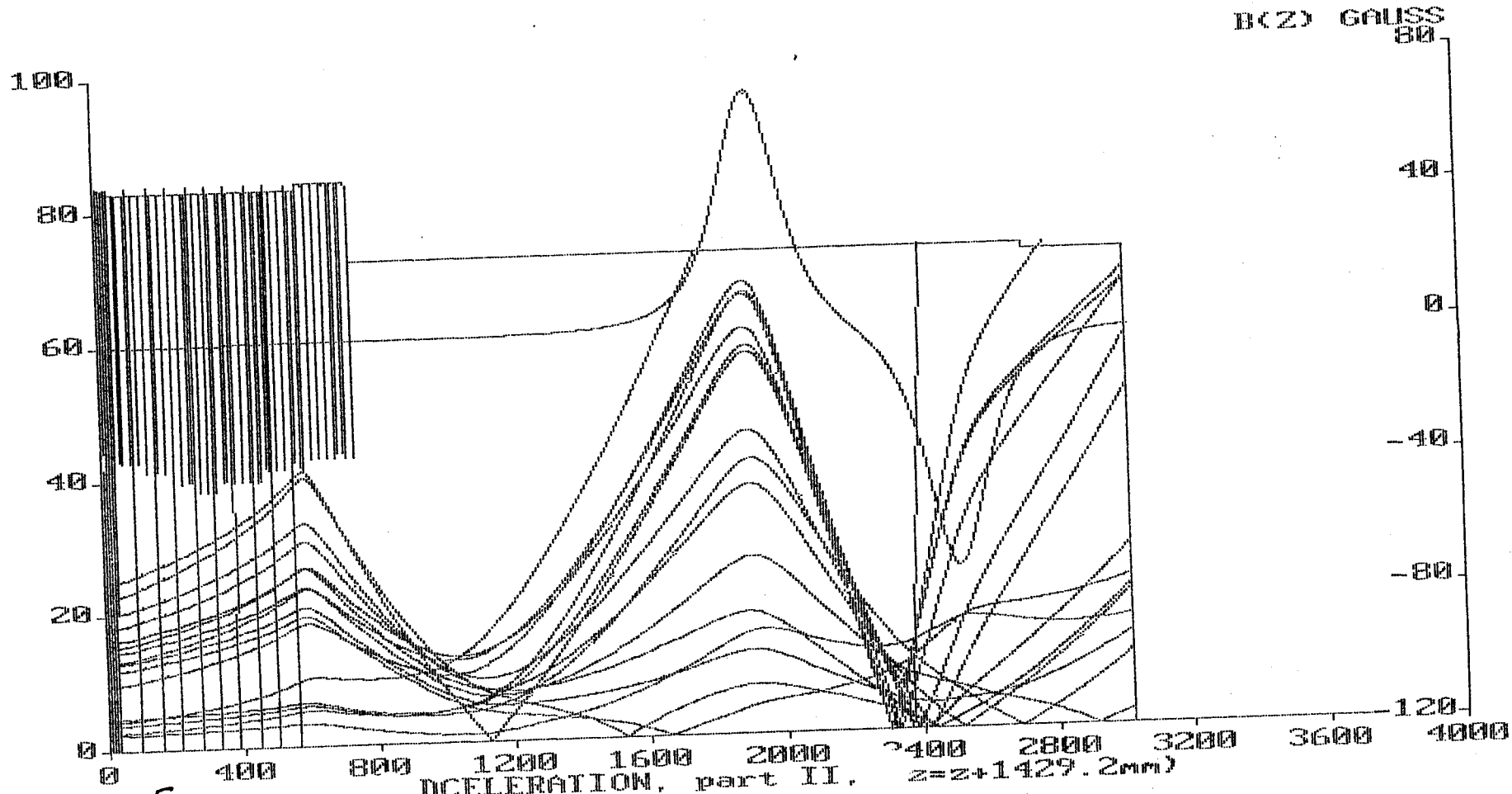
B(Z) GAUSS
80
40
0
-40
-80
-120
100
80
60
40
20
0
0
400
800
1200
1600
2000
2400
2800
3200
3600
4000
DCELERATION, part II. z=z+1429.2mm)

Fig. C4.

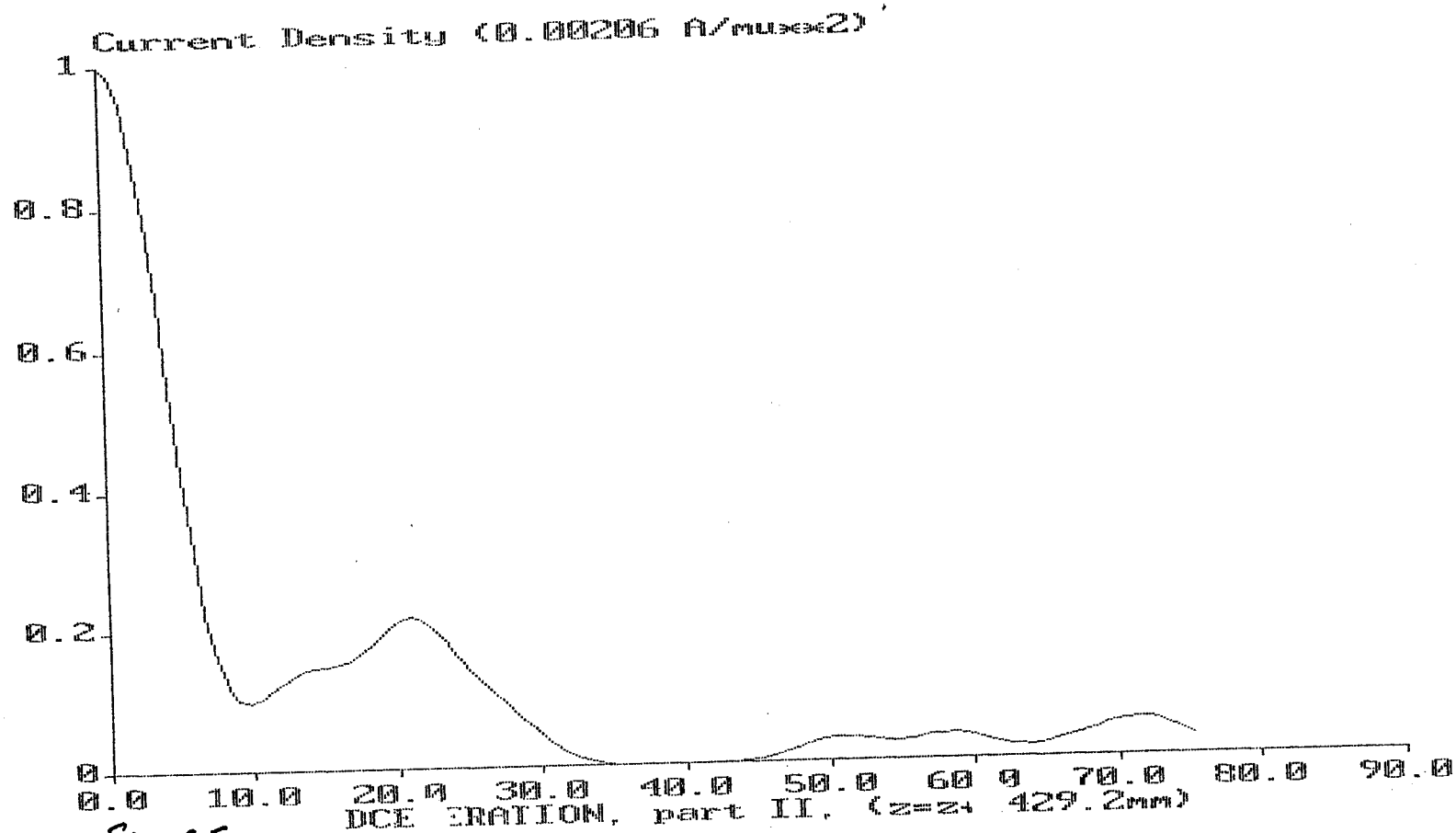
Current Density (0.00206 A/mu=<2)
1
0.8
0.6
0.4
0.2
0
0.0
10.0
20.0
30.0
40.0
50.0
60.0
70.0
80.0
90.0
DCE ERATION, part II. (z=2+ 429.2mm)

Fig. C5

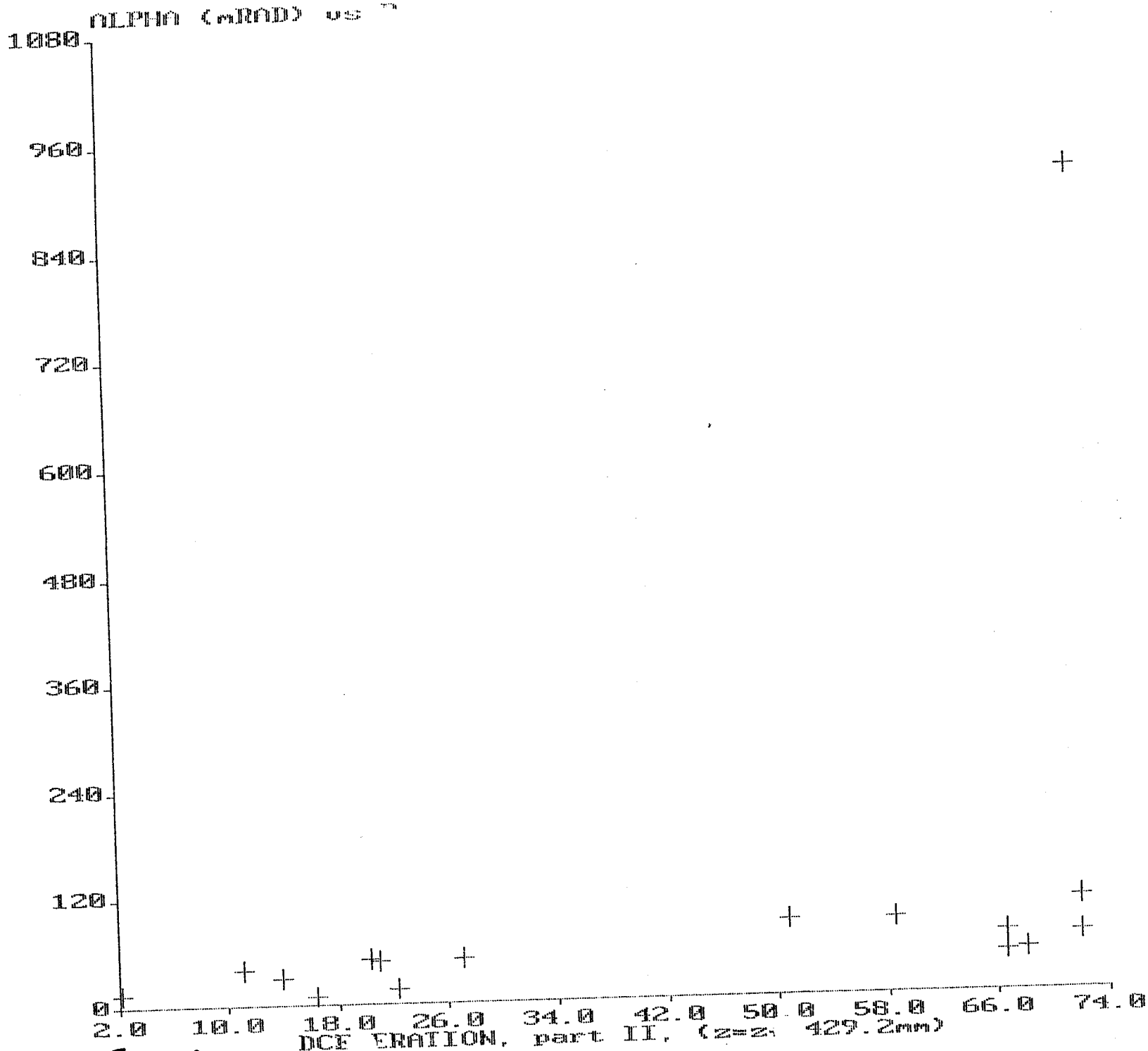
ALPHA (mRAD) vs
1080
960
840
720
600
480
360
240
120
0
2.0
10.0
18.0
26.0
34.0
42.0
50.0
58.0
66.0
74.0
DCF ERATION, part II, (z=z, 429.2mm)

Fig. C.6

21.12.97.

$I_1 = 4A.$

$I_2 = -4A.$

$U_\Sigma = 1445 kV$

$\Delta U_{collector} = 0.$

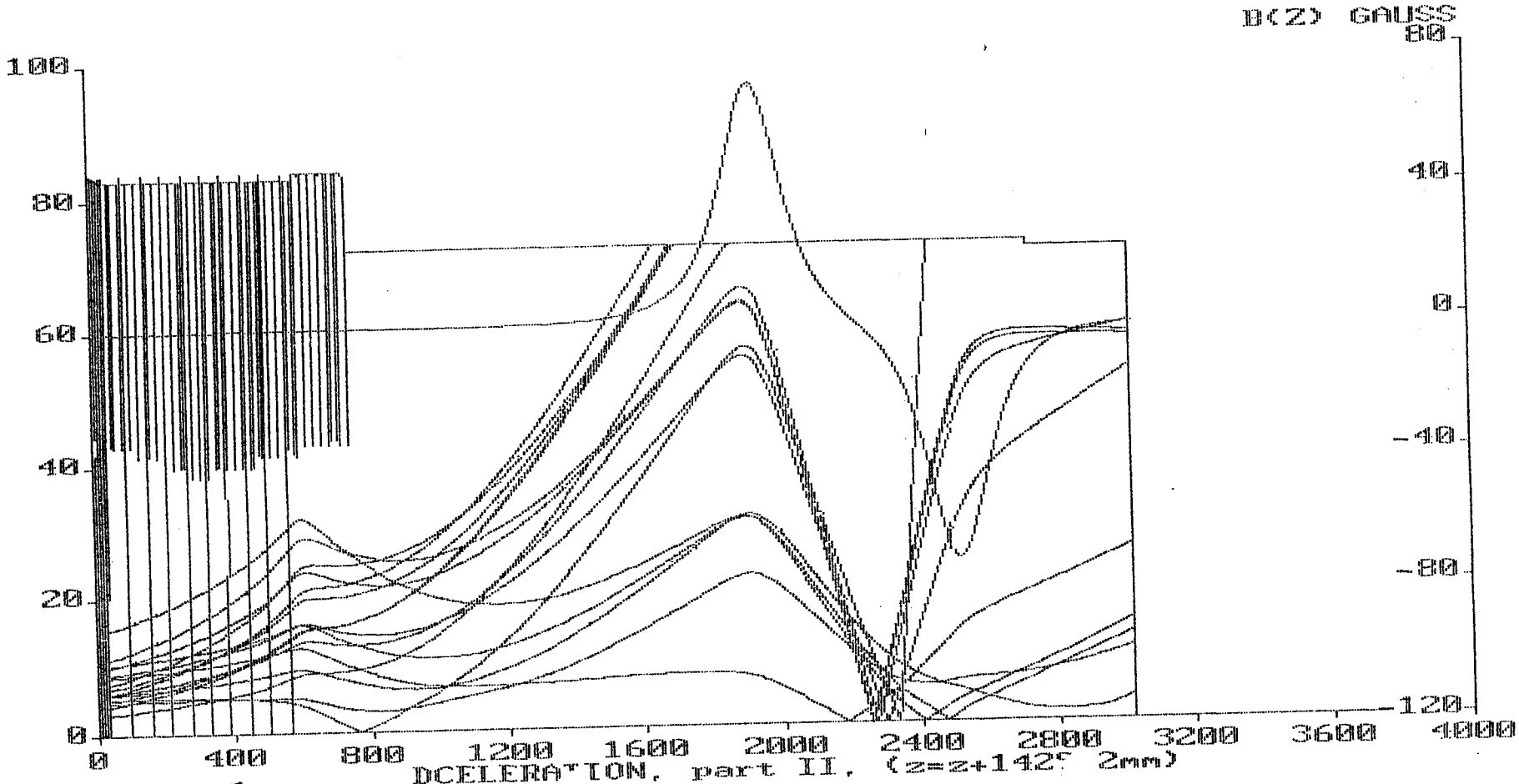

Fig. C7

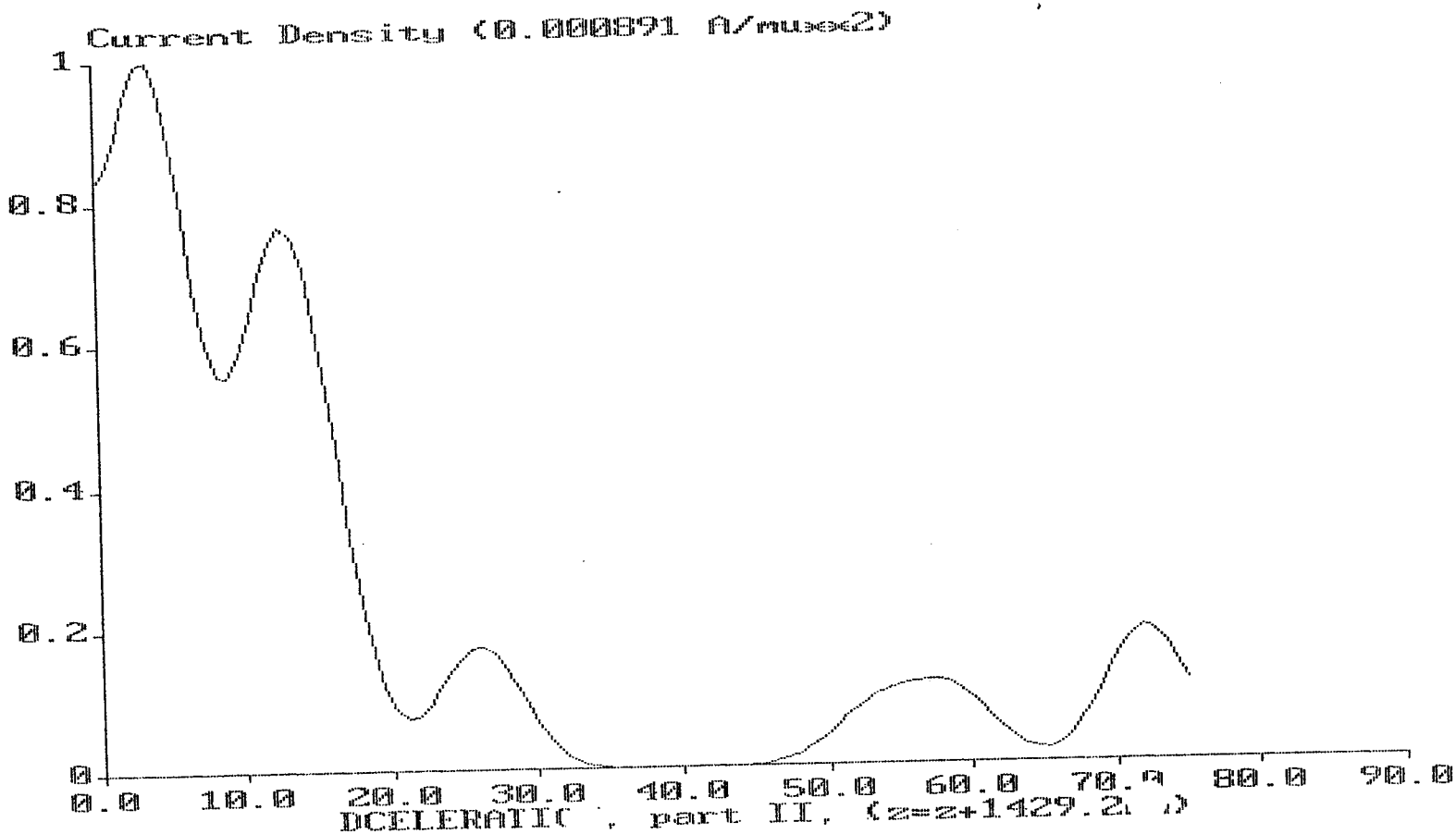
Current Density (0.000891 A/mu*m^2)
1
0.8
0.6
0.4
0.2
0
0.0
10.0
20.0
30.0
40.0
50.0
60.0
70.0
80.0
90.0
DCELERATIC , part II, (z=z+1429.2)

Fig. C8

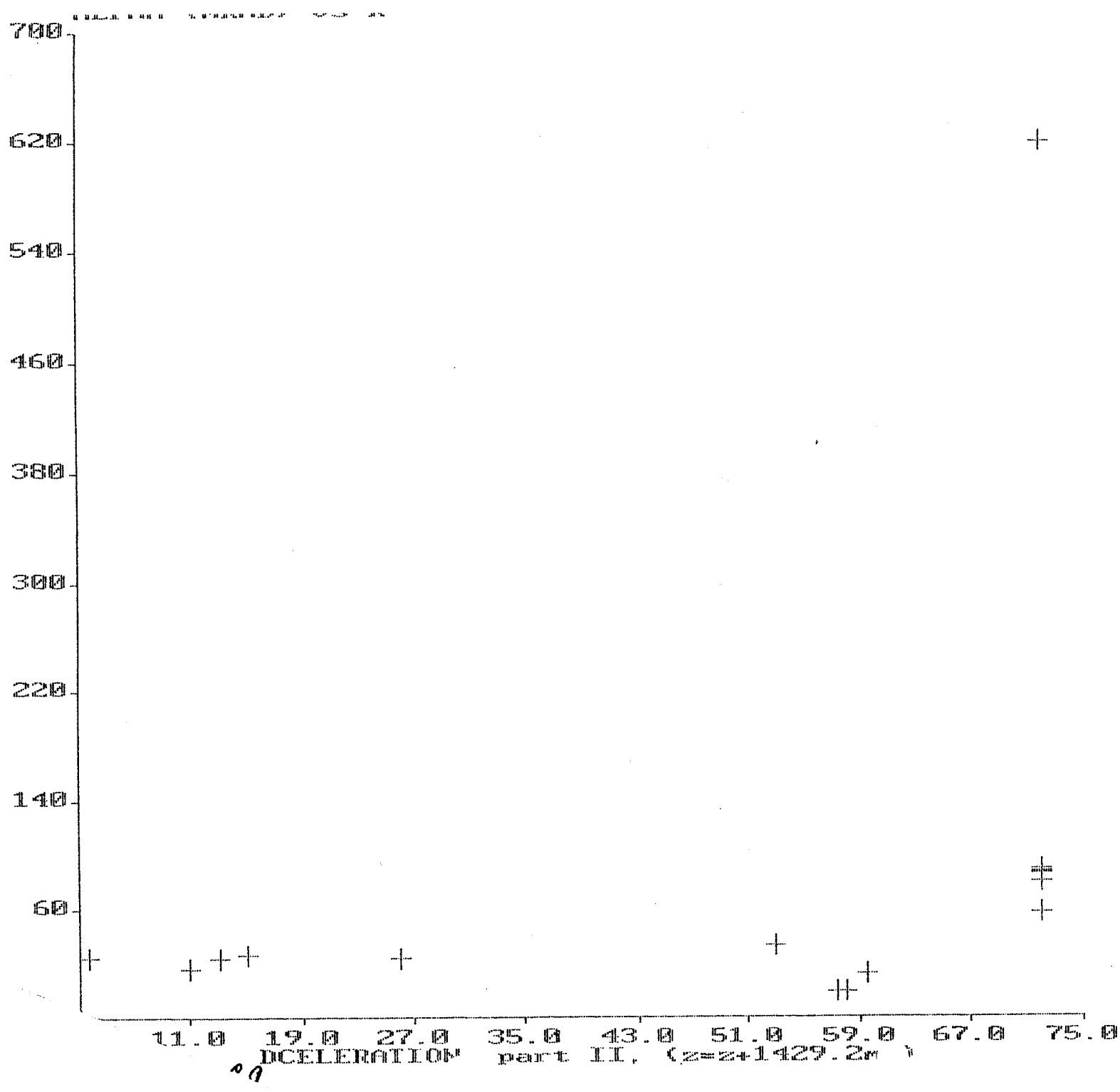
700
620
540
460
380
300
220
140
60
11.0
19.0
27.0
35.0
43.0
51.0
59.0
67.0
75.0
DCELERATION part II. (z=z+1429.2m